

IN VITRO TOOTH SHAPED SCAFFOLD CONSTRUCTION BY MIMICKING LATE
BELL STAGE

by

Pakize Neslihan Taşlı

Submitted to Graduate School of Natural and Applied Sciences
in Partial Fulfillment of the Requirements
for the Degree of Doctor of Philosophy
Biotechnology

Yeditepe University

2016

IN VITRO TOOTH SHAPED SCAFFOLD CONSTRUCTION BY MIMICKING LATE
BELL STAGE

APPROVED BY:

Prof. Fikrettin Şahin
(Thesis Supervisor)



Prof. Ahmet Arman



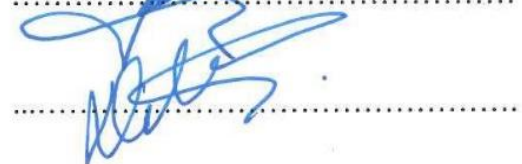
Prof. Ayşen Yarat



Prof. Figen Kaptan



Assoc. Prof. Dilek Telci



DATE OF APPROVAL:/.../2016

ACKNOWLEDGEMENTS

It is with immense gratitude that I acknowledge the support and help of my Professor Fikrettin Şahin. Pursuing my thesis under her supervision has been an experience which broadens the mind and presents an unlimited source of learning.

I thank Burçin Keskin and Research Assistants Ayşegül Doğan, Selami Demirci, Safa Aydın and Özge Sezin Somuncu.

Finally, I would like to thank my husband and my son for their endless love and support, which make everything more beautiful.

ABSTRACT

IN VITRO TOOTH SHAPED SCAFFOLD CONSTRUCTION BY MIMICKING LATE BELL STAGE

A key experimental trial in the regeneration of large oral and craniofacial defects is the neogenesis of osseous and ligamentous interfacial structures. Currently, oral regenerative medicine strategies are unpredictable for repair of tooth supporting tissues destroyed as a consequence of trauma, chronic infection or surgical resection. Here, this study shows mimicking immature tooth at the late bell stage design and construction of Hydroxy Apatite (HA) scaffolds for cell transplantation of human Adipose Stem Cells (hASCs), human Bone Marrow Stem Cells (hBMSCs) and Gingival Epithelial cells for the formation of human tooth dentin-pulp-enamel complexes *in vitro*. HA is the main factor that exist in tooth and it's in harmony with structural, biological, and mechanical characteristics. Scaffold characterization was demonstrated by SEM, FTIR and pore size and density measurements. The biological contraction of dental tissues against each other was demonstrated by mRNA gene expressions, histopathologic observations and protein release profile by ELISA technique. The newly formed tissue like structures that grow and integrate within the HA designed constructs forming tooth cementum like tissue, pulp and bone structures. This method suggests potential for the clinical application of personalized tooth constructs that may allow regeneration of multi tissue lines essential for oral, dental and craniofacial engineering applications.

ÖZET

DİŞİN GELİŞİMİNİ TAKLİT EDEREK DİŞ BİÇİMLİ HİDROKSİ APATİT İÇEREN GREFT YAPIMI

Ağız ve çene kemiği hasarlarının onarılmasına dair en önemli etkenlerden biri kemik, diş, ligament doku ve pulpa arasındaki yapıların oluşturulabilmesidir. Son zamanlarda diş doku mühendisliğinde kullanılan stratejiler, travmaya bağlı olarak zarar gören dokunun onarılması, desteklenmesi ve sterile edilmesine dayanıyor. Bu çalışmada diş oluşturmak için en önemli yapılardan olan dentin, pulpa, ligament ve enameli oluşturmak amacıyla gelişen bir diş taklit ederek içerisinde insan Adipoz Kök Hücre (iAKH), insan Kemik İliği Kök Hücre (iKİKH) ve diş eti epitel hücresi bulunan Hidroksi Apatit (HA) kaynaklı diş şeklinde bir greft inşa edilmiştir. Özellikle HA dişin yapısında bolca bulunan ve dişin yapısal, biyolojik ve mekanik içeriğini destekleyen bir moleküldür. Oluşturulan diş şeklindeki greftin karakterizasyonu SEM, FTIR analizleri ve por büyüklük ve yoğunluğunun ölçülmesiyle yapılmıştır. Hücrelerin birbirleriyle olan etkileşimlerini belirleyebilmek için mRNA seviyelerinin belirlenmesi, salgılanan proteinlerin ELISA yöntemiyle ölçülmesi ve histopatolojik olarak değerlendirilmesiyle belirlenmiştir. 8 hafta sonunda oluşan doku benzeri yapı HA greftle birleşip sementum, pulpa ve dentin benzeri yapılar gözlemlenmiştir. Klinik uygulamalarda, bu kişiye özel diş greftleri tasarlama, çoklu doku oluşturma ve ağız diş ve çene kemiği mühendisliğinde kullanılabilirliğini sağlayabilir.

TABLE OF CONTENTS

ACKNOWLEDGEMENTS	ii
ABSTRACT.....	iv
ÖZET	v
LIST OF FIGURES	viii
LIST OF TABLES.....	x
LIST OF SYMBOLS/ABBREVIATIONS.....	xi
1.1. STEM CELLS.....	1
1.1.1. Mesenchymal Stem Cells and Their Properties.....	2
1.2. ADIPOSE DERIVED STEM CELLS (ADSCs).....	3
1.3. TOOTH	4
1.3.1. Mammalian Tooth Development.....	5
1.3.2. The Role of Epithelium in Odontogenesis.....	7
1.3.3. Growth Factors Mediate Inductive Interactions During Odontogenesis	7
1.3.4. Role of Transcription Factors in Tooth Development	13
1.4. TISSUE ENGINEERING	15
1.4.1. Scaffolds That Used in Hard Tissue Engineering.....	17
1.4.2. Bioactive Ceramics	21
2. AIM OF THE STUDY	23
3. METHOD	24
3.1. SCAFFOLD CHARACTERIZATION	24
3.1.1. Preparation of Tooth-shaped Scaffolds and Cell Seeding.....	24
3.1.2. SEM	25
3.1.3. Porosity and Density Measurements.....	25
3.1.4. IR Spectroscopy	25
3.2. CELL CHARACTERIZATION AND SEEDING.....	26
3.2.1. Isolation and Characterization of hBMSCs, hASCs and Epitelial Cells	26
3.2.2. <i>In Vitro</i> Odontogenic Induction	27
3.2.3. ELISA	29

3.2.4.	Histopatology.....	29
3.2.5.	Immuno-histochemical Analysis	30
3.2.6.	Statistical Analysis.....	30
4.	RESULTS.....	31
4.1.	CELL ISOLATION AND CHARACTERIZATION	31
4.1.1.	Isolation and Characterization of Gingival Epithelial Cells (GECs).....	31
4.1.2.	ASCs isolation and Characterization	32
4.1.3.	BMSCs Isolation and Characterization.....	34
4.2.	Scaffold Characterization.....	35
4.2.1.	Porosity and density measurements.....	35
4.2.2.	SEM Images of Scaffold with and without cells	36
4.2.3.	FTIR.....	37
4.2.4.	Alizarin Red Staining of Scaffolds	38
4.3.	TOOTH CONSTRUCTION WITH HA HYBRID SCAFFOLD	38
4.3.1.	ELISA	38
4.3.2.	Histopatology.....	40
4.3.3.	Immunohistochemical Analysis.....	46
5.	DISCUSSION.....	49
6.	CONCLUSION	55
	REFERENCES	56

LIST OF FIGURES

Figure 1.1. Proliferation and differetion of Mesenchymal Stem	2
Figure 1.2. Schematic presentation of the developed tooth	6
Figure 1.3. Morphological changes in tooth development and the expression and use of transcription and growth factors	8
Figure 1.4. Wnt pathway at different stages of tooth development. Black; epithelium. Red; mesenchyme.....	11
Figure 2.1. In vitro tooth shaped construct demonstration	22
Figure 2.2. A flow chart of process steps for scaffold fabrication using combined Agarose and NaCl methods.....	24
Figure 4.1. a.Primary gingival epithelial cell light microscope images (5x, 20x). b. Epithelial cell specific antibody staining (EpCAM, Epithelial Antigen) (5x)	31
Figure 4.2. Characterization of fat derivative stem cells. a. Adipose stem cell image. 10X. b. Stem cell characterization of cell derived from fat tissue.....	32
Figure 4.3. Odontogenic differentiation of hASCs. (a) Alizarin Red Staining,(b) Alkaline Phosphatase (ALP) Activitiy of cells, (c) Real-time polymerase chain reaction analysis: relative messenger RNA expression of COL1A and dentin sialophosphoprotein (DSPP), NC, nontreated cells; PC, odontogenic medium only. Scale bars = 100 μ m.	33
Figure 4.4. a. Stem cells from jaw bone marrow. 10X. b. Human bone marrow stem cell characterization, isolated from mandibular bone.....	34

Figure 4.5. SEM images show the porous structure of HA hybrid scaffold with open and connective form. SEM images of interconnected porous of HA scaffold prepared with mixture containing 40 wt % HA (b) with and (a) without cells.	36
Figure 4.6. Light Microscopy image of interconnected porous HA scaffold prepared with slurries containing 40 wt% HA (a) 200X, image of HA scaffold stained with (c) Alizarin Red Stain with and without (b) odontogenicly differentiated cells	37
Figure 4.7. FTIR spectra of HA scaffolds. Figure shows difference between (black line) HA.....	38
Figure 4.8. Relative FGF 3, FGF 10 and BMP 4 proteins release from cells seeded on tooth shaped scaffolds for 8 weeks	40
Figure 4.9. H&E stainings of 0 th week sections	41
Figure 4.10. H&E stainings of 4 th week sections.....	42
Figure 4.11. H&E stainings of 8 th week sections.....	43
Figure 4.12. TCM stainings of 0 th , 4 th and 8 th week sections.....	44
Figure 4.13. Specilized structures of cells seeded on HA hybrid scaffolds.....	45
Figure 4.14. Time dependent immunohistochemical staining of tooth formin cells. Used antibodies are BMP 2, 4,7, FGF 3, Msx 1	46
Figure 4.15. Time dependent immunohistochemical staining of tooth forming cells. Used antibodies are DMP 1, DSPP, Amelogenin and VEGFR	48

LIST OF TABLES

Table 1.1 Main features of scaffold that used in tissue engineering.....	28
Table 1.2. Physical properties of synthetic, biocompatible, and biodegradable polymers used as scaffold materials.....	30
Table 1.3. Mechanical features of bioactive ceramics.....	32
Table 3.1. RT-PCR reagents.....	40
Table 3.2. RT-PCR conditions.....	40
Table 4.1. Density and porosity values at changing HA concentrations.....	47

LIST OF SYMBOLS/ABBREVIATIONS

ADSCs	Adipose derivative stem cells
ALP	Alkaline phosphatase
ATR	Attenuated total reflectance
COL1A	Collagene type 1
Dkk	Dickkopf
DMEM	Dulbecco's modified eagle's medium
DSPP	Dentin sialophospho protein
DXM	Dexamethasone
ECM	Extracellular matrix protein
EdaA1	Ectodysplasin A1
EDARADD	EDAR and EDAR death domain adaptor
EtOH	Ethanol
ESCs	Embryonic stem cells
FBS	Fetal bovine serum
FTIR	Fourier transformed infrared
HA	Hydroxy apatite
HCA	Carbonated hydroxy apatite
Hh	Hedgehog
IKB	Inhibitor of κ B
IKK	IKB kinase
LDL	Low density lipoprotein
MSCs	Mesenchymal stem cells
PGA	Poly glycolic acid
PHA	Poly-hydroxy-alkanoates
PHB	Poly-3-hydroxybutyrate
PHBV	Copolymers of 3-hydroxybutyrate and 3-hydroxyvalerate
PLA	Poly lactic acid
PLGA	Poly lactic-coglycolic acid
Ptc	Patched

SCs	Stem cells
sFrp	Frizzled related protein
Shh	Sonichedgehog
Smo	Smoothed
TNF	Tumor necrosis factor
TRAF 6	TNF receptor-associated factor 6
VEGF	Vascular endothelial growth factor



1. INTRODUCTION

1.1. STEM CELLS

The self renewal and multilineage differentiation ability of Stem Cells (SCs) makes them favorable agent for regeneration and tissue reorganization studies. They can be obtained from almost every type of tissue and they are defined by their sources such as Embryonic Stem Cells (ESCs) have potential to form whole organism, mesenchymal derived stem cells have multi- and pluripotency that ability of differentiate many type of cell.

SCs are individuated from other cell types by these several important characteristics:

- SCs are undifferentiated cells, capable of regenerating themselves during cell split,
- They can be harvested by a minimal invasive procedure
- They can be used transplanted studies without any immunologic reaction, its providing safe and effective usage for living organism,
- They can be found in abundant quantities (depends on their source)
- Under optimal environments, they can be turned into tissue- or organ-specific cells.

SCs can be obtained from two main sources; embryonic blastocyte and adult tissue. Embryonic stem cells are derived from the early mammalian embryonic blastocyte and they can give whole organism [1].

ESCs obtained from the inner cell mass of blastocysts have the potential to become a multiplicity of dedicated cell types [2]. ESCs have regenerative potential and pluripotency, they can differentiate into ~220 kinds of cell types found in the organisms.

Adult stem cells are taken from different tissues of the developed organisms. Adult organisms remain this undifferentiated, or unspecialized, state. These adult stem cells can be turned into many type of cell. Recently these cells can be used as main implantation factor.

1.1.1. Mesenchymal Stem Cells and Their Properties

Mesenchymal Stem Cells (MSCs) can be found almost from every type of tissue such as bone marrow, lung, adipose tissue, dental tissues, cord blood and various fetal tissues [3]. MSCs are post-embryonic adult stem cells and they can turn into many cell types in the body, including osteocyte, odontocyte, chondrocyte, myocyte, and adipocyte when optimal conditions are provided. For instance for odontogenic differentiation the cells must be treated with inductive chemicals, cytokines and growth factors [4]. Recently, scientists interested in tissue engineering studies, for bone, tooth, skin and cartilage repair [5, 6].

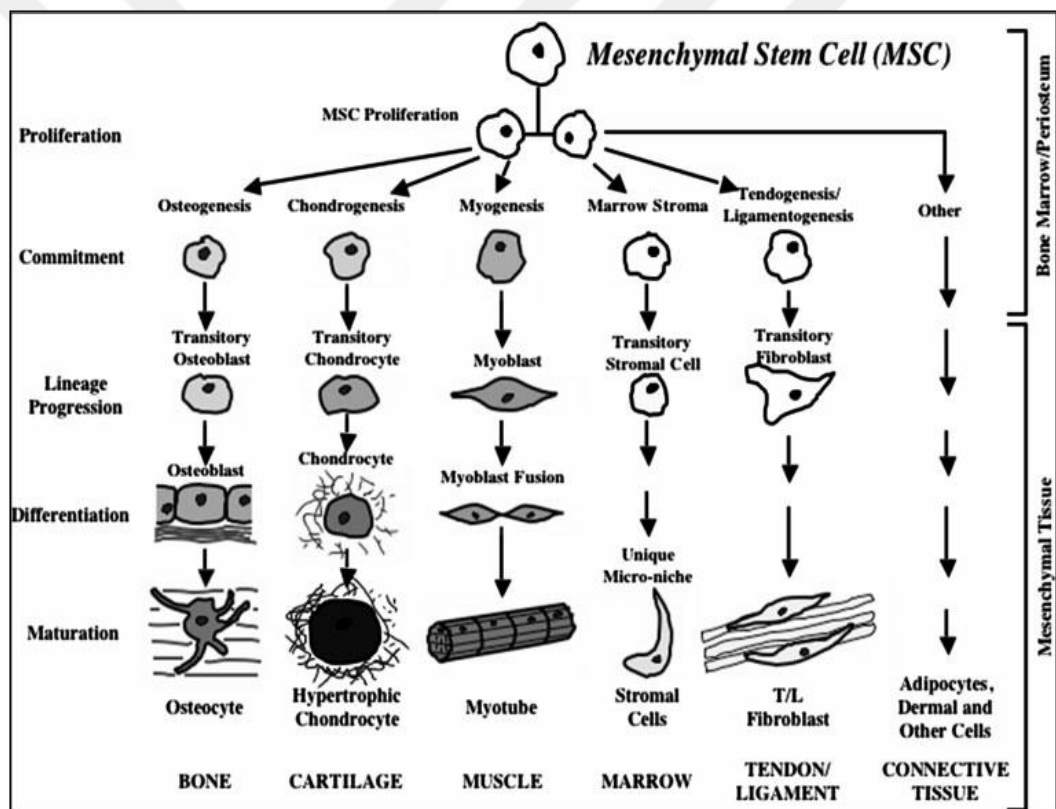


Figure 1.1. Proliferation and differentiation of Mesenchymal Stem [7].

The first successful mesenchymal stem cell isolation is the fibroblast like colonies from the bone marrow, reported by Friedenstein [8]. The isolation technique was based on the attached marrow-derived cells which fibroblast like cells adhere to a plastic surface of the

cell culture plate, with a concomitant lack of attachment shown by the marrow derived hematopoietic cells [9, 10].

According to the criteria of The International Society for Cellular Therapy, MSCs are characterized by their surface markers which should be negative for the hematopoietic cells surface markers such as CD14, CD34, CD45 [11-13] and be positive for the MSCs surface markers such as CD105, CD73, and CD90 [3]. The phenotypic characteristics of MSCs are not specific, these features are shared between multiple cell lineages, including the mesenchymal, hematopoietic, endothelial, epithelial, and muscle cells [14, 15]. In addition to these characteristics, MSCs have show a multiple of phenotypic features [12]. In the tissue engineering studies, they can be cultured with other cell types and implanted to variety of organisms but these applications may alert immune system of host organism. To prevent host defense system, immunosuppressive capacities of MSCs have been studies in experimental autoimmune models [16]. Zappia and colleagues [17] were the first to report the therapeutic efficacy of MSCs in the experimental autoimmune murine model of the multiple sclerosis (MS).

1.2. ADIPOSE DERIVED STEM CELLS (ADSCS)

MSCs obtained from the bone marrow stroma have been proposed as an ideal source. They are famed as a main source of osteogenic stem cells. MSCs differentiate into adipocytes, chondrocytes, osteoblasts, and myoblasts *in vitro* [18, 19] [20] and *in vivo* [21, 22], these features making them hopeful candidates for tissue engineering applications. Nevertheless, the clinical usages of MSCs have showed some problems, such as pain, morbidity, and low cell number leading harvest. To achive this problems, scientists had to investigate alternative MSCs sources.

As an alternative source, fate tissue is obtained from the mesenchymal part of the tissue and it contains a supportive stroma. The main features of stromal cells are consisting of the capacity to attachto plastic surface to form fibroblastic-like morphology, the ability to express stem cell surface antigens, and the ability to differentiate into several mesodermal cells, including bone, cartilage, muscle, epithelium, fat and neural progenitors. Because of

these characteristics, adipose derived stem cells (ADSCs) have potential to be useful in the field of regenerative medicine studies. The advantages of adipose tissue are cheaper than bone marrow, with less complicate operation and obtainable in greater quantities. ADSCs, extracted from isolated adipose tissue, shows higher stem cell proliferation rate than BMSCs. Hence, adipose tissue represents a plentiful, useful, and attractive source of donor tissue for autologous cell implantation studies. The successful application of ADSCs on regeneration therapy can be achieved just after; extensive characteristics are learned in details.

ADSCs have multifaceted signal flow of transcriptional and non-transcriptional movements that occurs all over the body. Differentiation of adipogenic cells is a complex process complemented by synchronized deviations in cell morphology, hormone sensitivity and gene expression that have been studied mostly in murine pre-adipocytes. While historically in the literature, ADSCs have been defined as a “pre-adipocytes”, there is a rising admiration that they have multipotency, with chondrogenic, neurogenic and osteogenic capability. Additionally, recent studies have shown that adipocytes differentiate from the neural crest *in vivo* and *in vitro*, thus providing important approaching into the developmental origin of the adipocyte lineage. This opens new opportunities to study tissue engineering applications.

1.3. TOOTH

In vertebrates tooth organ growth, from the initiation to terminal differentiation, depends leading inductive cell to cell interactions typically between epithelium and dental mesenchyme [23, 24].

These inductive cell to cell interactions consist of two main factors:

- a tissue be able of producing the inductive signals and
- a tissue be able of receiving and responding to it.

These interactions include variety signaling networks composed of different signaling molecules, their receptors, and the expressional control systems. Most of these signaling molecules known as a growth factors and some are Bone Morphogenetic Proteins (BMPs),

Fibroblast Growth Factors (FGFs), Wnt, and Hedgehog (Hh) families. These molecules have function to organize and guide tissues and organs during development. Transcription factors in a tissue layer trigger the expression of these growth factors in response to the expression from the adjacent tissue, forming a signaling set-up that controls organogenesis [25].

Tooth growth shares many similarities with other embryonic organs. The murine tooth has big potential that serve as a model tissue for studying essential questions of developmental cell to cell interactions such as epithelial-mesenchymal relation, differentiation, and formation. In the fields of clinical applications, tooth allo-, autotransplantations, and dental implants have been usually used as general procedures for tooth replacement method for many years. Even though damaged dental tissues are not critical effects the quality of human's life. MSCs mediated tissue engineering methodologies to replace organ and tissue for the clinical application become very hopeful [26].

1.3.1. Mammalian Tooth Development

In mammalian sequential and reciprocal connections between the neural crest derived mesenchymal cells and the stomadial epithelium control tooth morphogenesis and differentiation [27]. Stages of tooth development: initiation, bud formation, cap formation, bell formation, apposition, maturation, root formation and eruption. In murine, the forming of tooth sites and shape happens around embryonic day 10.5. At embryonic day 11.5, the first morphological mark of molar tooth shows up as an initiation stage. At this stage, the presumptive dental epithelial cells extend along their apical-basal axis, change cell shape from cuboidal to columnar. At the embryonic day 12.5 and embryonic day 13.5 bud stage, the condensed dental epithelium cells proliferate and immigrate into the subjacent mesenchyme to shape the epithelial tooth bud.

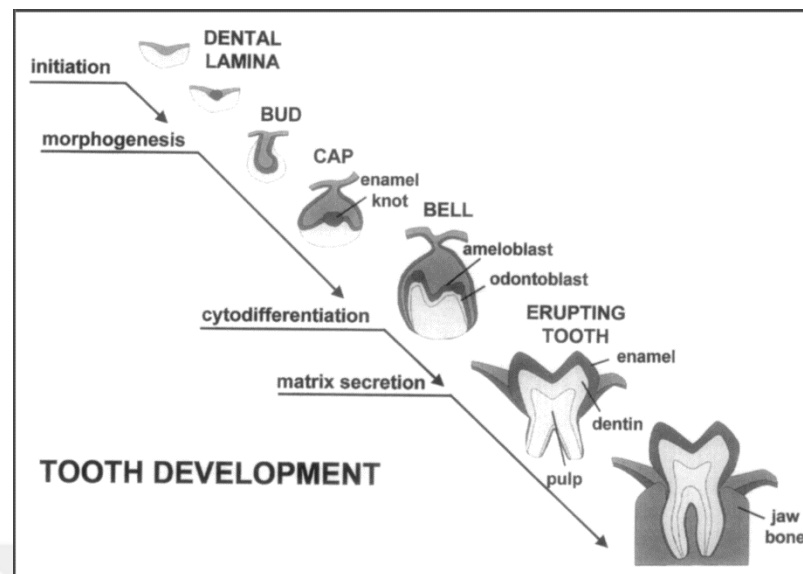


Figure 1.2. Schematic presentation of the developed tooth [28].

At the embryonic day 14.5 cap stage, proliferation of the dental lamina into a small, rounded structure overlying on area of condensing connective tissue, the epithelial part shows specific folding, which is accompanied by the configuration of the enamel knot. The enamel knot working as a signaling center, it is express set of signals, including Shh, BMP 2, BMP 4, BMP 7, FGF 4, and FGF 9 [28]. During the bell stage, further growth of the bud that becomes indented and covers the dental papilla; the epithelial derived ameloblast and mesenchymal derived odontoblast cells of the cap are differentiated. During apposition stage, formation of the crown by dentinogenesis and amelogenesis with the deposition of dentin protein (collagen) and enamel protein (amelogenin) and the beginning of calcification are started; preameloblasts, from the inner enamel epithelium, induce adjacent cells of the dental papilla to become odontoblast that then produce the dentin matrix which in turn induces the preameloblasts to become ameloblasts that produce enamel matrix. Tooth maturation include the completion of the crown by further deposition of the enamel and completion of calcification; at the cervical area is an extension of the inner and outer enamel epithelium forming a bilayered root sheath that will induce the formation of the root. The root forms as the tooth erupts; the epithelial root sheath induces odontoblasts to form root and then it disintegrates allowing cells from the dental sac to become cementoblasts, aligning next to the producing cementum matrix that will calcify into cementum; cells from the dental sac also can tribute to formation of the periodontal ligament.

1.3.2. The Role of Epithelium in Odontogenesis

To understand the effective role of epithelium on tooth formation, scientists focused on investigation the interaction between epithelium and ectomesenchyme, in tooth morphogenesis and importance of enamel knot. The interaction between homeobox genes in patterning, transcription factors that control the activity of other genes and the various families of cytokines are reveal importance of epithelium. Main transcription factors are expressed in dental epithelium, and these genes in the ectomesenchyme which expresses further intercellular modulatory molecules and other homeobox genes essential for tooth development [24]. The role of epithelium in the initiation of odontogenesis at the tooth development cannot be ignored.

1.3.3. Growth Factors Mediate Inductive Interactions During Odontogenesis

Recent studies have shown the significance of cell to cell interactions between dental epithelium and dental mesenchyme during tooth development. Parts of embryonic mouse tooth germs, epithelium or mesenchyme are unsuccessful to differentiate, and the epithelium dies after isolation [29]. On the other hand, physical separation with filter epithelium and dental mesenchyme starts to form enamel organ and papilla with the deposition of matrix proteins. These studies showed that the cell to cell interactions between these two parts are needed for their differentiation or survival, and the interactions are regulated by simulative signaling molecules. It is clear that these simulative signaling molecules are growth factors.

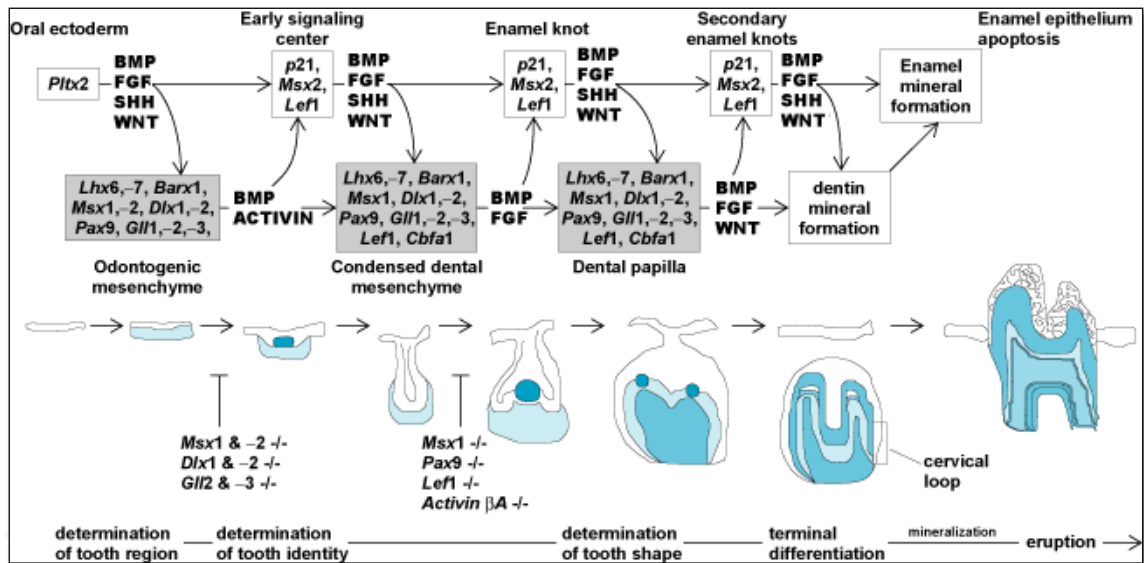


Figure 1.3. Morphological changes in tooth development and the expression and use of transcription and growth factors [30].

1.3.3.1. BMPs

Recent studies have shown that BMPs are important for mammalian tooth organ generation, even the expression of many BMP genes in tooth development has been reported in many studies, and for example, *Bmp 4* plays a critical role during tooth development [28]. During the cap stage, epithelial cells expressed *Bmp4* and *Fgf8* restrict *Pax9* expression to the future dental mesenchyme [31-33] and the expression of *Pitx2* to epithelium [34]. To example of regulatory roles of *Bmp 4*, that is expressed in the distal site of mandible, is restriction of transcription factor *Barx 1* expression to future molar [32, 35] and induction of *Islet 1* expressed from the future incisor mesenchyme [36].

During the initiation stage many growth factors are expressed from the condensed epithelium. Some of these are *Fgf 8*, *Fgf 9*, *Bmp 2*, *Bmp 4*, *Bmp 7*, *Shh*, *Wnt10a*, and *Wnt10b* [37-41]. These expressed growth factors regulate and stimulate gene expression in the adjacent dental mesenchyme, including *Msx 1*, *Msx 2*, *Lef 1*, *Dlx 1*, *Dlx 2*, *Patched (Ptc)*, *Gli 1*, and *Syndecan 1* [41-44].

At the bud stage, these inductive molecules stimulate gene expression in the dental mesenchyme, including Bmp 4, Fgf 3, activin- β A, and Wnt5a [37, 45-47]. At this stage these inductive growth factors provide odontogenic characteristic to dental mesenchyme.

During the cap stage of developed tooth, a series of specific molecules started to express including Bmp 2, Bmp 4, and Bmp 7 are from the enamel knot which plays role as signaling center. Recent studies were shown effective role of Bmp 4, it was given to dental mesenchyme this lead to morphogenic changes and inducing expression of transcription factors, including Msx1, Msx2, Lef1, and Egr1 in the dental mesenchyme [37, 42]. Additionally, it was shown that mesenchymally expressed Bmp4 responsible for the induction and maintenance of gene expression, such as Shh and p21, in dental epithelium [48, 49].

Bmp 2, Bmp 4 and Bmp 7 expressed from enamel knot, may be cause for apoptosis in the knot cells . BMPs have two type receptor, one of them is type BMPR1 including BMPR1A and BMPR1B and the other one is type II BMPR2 [50]. Firstly, BMPs bind to their receptors; activated BMPR2 phosphorylates the BMPR1 which in turn phosphorylates the DNAbinding proteins Smads and enter to nucleus site to modulate the gene activation [51]. Both type I BMPR1 receptors are expressed in early developing tooth germ [52]. Studies were shown that BMPR1A deficient mice die before tooth formation [53], but BMPR1B deficient mice do not reveal any defect in teeth form [54, 55]. These studies implying that BMP signaling is necessary for the growth of tooth from the initiation to the eruption stage [42].

1.3.3.2. FGFs

FGF family that play important role on odontogenesis from initiation stage to the formation of the bell stage, are expressed in the early forming tooth germ [30]. Expression of Fgf 8 and Fgf 9 were shown in the dental epithelium, expression start to tooth initiation stage to early bud stage.

FGF signaling participates in restricting tooth forming sites by inducing the expression of [31, 33, 34]. Fgf 8 is responsible for the restriction gene expression in the tooth forming sites such as Pax 9, Pitx 1, and Pitx 2 and induction of Barx 1, Lhx 6 and Lhx 7 in the molar mesenchyme to the initiation and rest of the stages. Fgf 9 was stimulating the enamel knot and the Fgf 4 was activated by Wnt signaling, at the late bud stage and the early cap stage and they induce cell proliferation of both epithelium and dental mesenchyme [40, 56, 57]. In addition Fgf 8 may play role for the stimulation of Fgf 3 expression in the dental mesenchyme. Fgf 3 and Fgf 10 expressed from dental mesenchyme at the bud stage. While Fgf 3 can stimulate cell proliferation in isolated mesenchyme [47]. Some studies showed that Fgf 3 and Fgf 10 deficient mice didn't exhibit important tooth defects [58-60].

1.3.3.3. *Shh*

Sonic hedgehog (Shh), a member of the vertebrate Hh family, encodes a secreted signaling peptide and it is the only Hh family ligand to be expressed during the tooth development. When Shh receptor activated by the ligand, cell started to response by activating secondary protein that is Smoothened (Smo). Activation of secondary protein Smo leads expression of Ptc 1 and Gli 1, by activating transcription. Even though single knockout of the three Gli genes did not show obvious tooth defects.

Double mutants of Gli 2 and Gli 3 caused abnormal growth at the bud stage [39]. Thus Shh signal interactions are required for early tooth growth. Shh signaling molecules are found in the epithelium at the dental lamina stage until cells start to differentiation [38] [61, 62] [63]. Shh expression is controlled by enamel knot [61] [39].

During the cap stage Shh signals including Ptc 1, Gli 1 and Smo are expressed from dental epithelium, and regulate initiation stage and bud formation by inducing epithelial cell proliferation [39, 64].

At the end of the bud stage Shh expressed not only in the enamel knot also spreads to the inner enamel epithelium and the stratum intermedium cells during the tooth development stages [61, 62, 65]. Smo deficient mice studies demonstrate that lack of Smo causes

abnormally fusion of the first and second molars in both the maxilla and mandible, the same results observed in *Shh* knockout mice [66].

1.3.3.4. *Wnts*

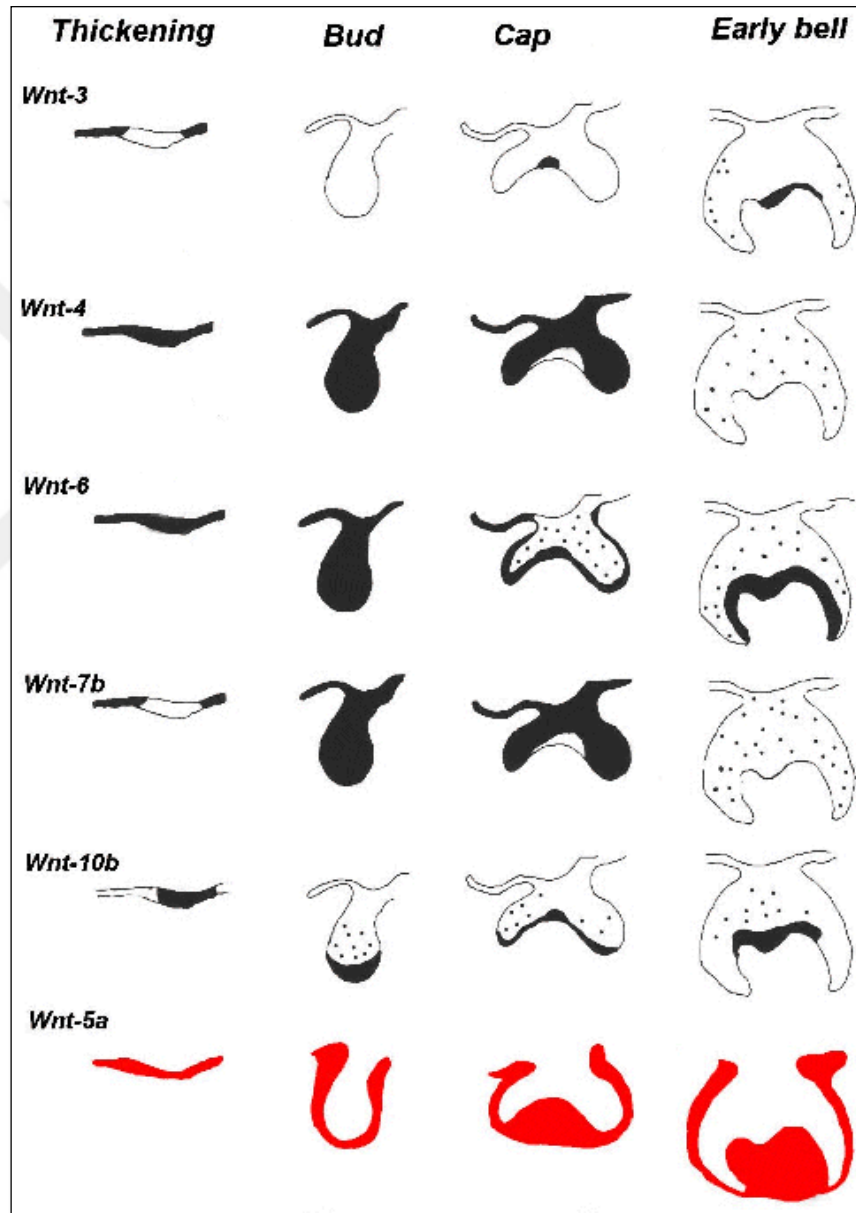


Figure 1.4. Wnt pathway at different stages of tooth development. Black; epithelium. Red; mesenchyme [46].

Wnt family has wide and diverse kind of signaling molecules responsible for morphology, proliferation and differentiation of a many of tissue and organs [67]. One of the Wnt signal family member is related to Frizzled receptor family [68-70]. Other member of Wnt family is related to the low density lipoprotein (LDL) receptors and defined as a LRP5/6 [71, 72]. Wnt signal molecules can bind to both LRP5/6 and Frizzled to activate the canonical Wnt/ β -catenin and planar cell polarity pathway [73]. WNT antagonists play important role on regulation of these signals. These antagonists Frizzled related protein (sFrp) family have functioned as soluble regulators of Wnt signaling [74-76]. Another one is Dickkopf (Dkk) family; they are acting as inhibitory ligands of LRP5/6 co-receptors. Dkk molecules bind to LRP5/6 receptors and block the cell response, but the Wnt-Frizzled complex can be still active. Therefore, Dkk can block the canonical pathway but it cannot be inhibit planar polarity pathway.

Most of Wnt signaling molecules are expressed in the dental epithelium, but few expressed in the dental mesenchyme in developing tooth. Wnt7b is expressed in dental epithelium and ectopic expression of Wnt7b causes inhibition of expression of Shh signal molecules and afterward inhibits tooth formation, but not vice versa. Also, Wnt7b effects interaction of ectodermal margins between oral and dental ectoderm, by inhibiting Shh signaling [77].

Wnt10a and Wnt10b are expressed in dental epithelium it starts at the initiation stage and remain until eruption [78]. At the cap stage, both Wnt10a and Wnt10b genes are expressed from the enamel knot.

Wnt 4 and Wnt 6 were expressed in the dental epithelium too; on the contrary, sFrp 2, sFrp 3 and Wnt 5a, are expressed in the dental mesenchyme [46]. The first study about role of Wnt signaling in tooth growth was demonstrated that Lef1 knockout mice cannot develop fully grown teeth [43, 57, 79]. sFRP 3 treatment to the cultured molar region showed abnormal tooth bud formation after the *in vivo* transplantation [80]. Another study showed that over-expression of Wnt3 in the epithelium did not effect of tooth morphology [81]. But knockout mice for many Wnt genes, including Wnt 1, Wnt 2, Wnt 3, Wnt 3a, Wnt 4, and Wnt5a, were died too early for morphological tooth analysis or do not showed any kind of tooth phenotyping [67, 82, 83].

1.3.3.5. *TNFs*

As a signaling center enamel knot effect directly tooth phenotype and growth [30]. This supported by the proofs obtained from the Tumor Necrosis Factors (TNF) signal pathway studies. Several mutant studies exhibit some facts related tooth development, some of them Tabby, Downless and Crinkled [84-87]. Tabby is defined as Ectodysplasin A1 (EdaA1) and expressed from outer enamel epithelium. Downless and Crinkled are defined as TNF receptor EDAR and EDAR death domain adaptor (EDARADD) [85, 88, 89] and expressed from enamel knot [90-92]. All three mutants showed abnormal tooth formation [85, 88, 90]. Furthermore, addition of EDA protein to pregnant Tabby mice shows renormalization tooth structure [93], but over-expression of EDAR in the epithelium leads to abnormal tooth structure [94]. These findings demonstrated that molar structure is modulated by the EDA signaling [95]. Also, EDA signaling pathway involves a kinase cascade leading to activation of nuclear factor kappa B (NF- κ B) [96-98]. Active form of NF- κ B is regulated by inhibitor of κ B (IKB) that is regulated by IKB kinase (IKK). IKK have one modulatory IKK γ , and two activator IKK α and IKK β subunits. The expression of NF- κ B, Ikb and Ikk γ are expressed from the enamel knot, at the cap stage. Ikk α knockout mice show the same results with the Eda, Edar, and Edaradd mutant mice studies [99]. TNF receptor-associated factor 6 (TRAF6) mediate to activated NF- κ B by the EDA signaling [100]. Many Trafs is expressed by dental epithelium [101] and its absence lead more abnormal structure than knockout Eda/Edar/Edaradd studies [100]. These findings show the importance of the TNF signaling pathway in forming of molar morphology.

1.3.4. Role of Transcription Factors in Tooth Development

1.3.4.1. *The homeobox-containing genes*

Mouse studies shown that physiological form of tooth development depends on special expression pattern of a number of homeobox genes, such as Pax 9, Msx 1, Msx 2, Dlx 3, Dlx 5, Dlx 6, Dlx 7, Barx 1, Pitx 2, Lhx 6, Lhx 7 [102, 103]. Barx1 expressed from molar

mesenchyme at the tooth formation and it has role on determination of molar tooth type [35]. Its expression regulated by BMP 4 and FGF 8 [32]. Barx1 knock down mice studies showed Barx1 has importance role on the development of molar tooth germ.

The expression of Msx 1 and Msx 2 is detected in the developing tooth germ in patterns that correlate with morphogenetic steps in tooth development [104]. Msx 1 and Msx 2 are expressed from the dental mesenchyme at the initiation, bud, cap and bell stages of tooth development. Component of Msx 2 also expressed to the dental epithelium and enamel knot. Knockout Msx 1 studies demonstrated that Msx1 is necessary for tooth viability, but Msx2 knockout mice exhibit structural abnormalities [105, 106]. Lack of Msx1 in Msx1 knockout mice showed down regulation of some genes, including Bmp 4, Fgf 3 and Lef 1 [41, 42, 44]. BMP4 treatment to the knockout Msx1 mice somewhat rescued Msx 1 mutant tooth phenotype [42, 49, 107].

Pax 9 is a member of paired domain family genes and it is expressed in the dental mesenchyme. Active BMP and FGF regulate expression of Pax 9 in the dental mesenchyme [31]. Also, Pax 9 deficiency leads down regulation of variety genes such as Bmp4, Msx1, and Lef1 in the dental mesenchyme [108]. Pax 9 and Msx 1 control BMP 4.

FGF 8 up regulates the Pitx 2 expression, while BMP 4 down regulates, in the dental epithelium [34, 109]. Additionally, Pitx 2 deficiency leads down regulation of Fgf 8 in the dental epithelium [110], showing that expression of Pitx 2 and Fgf8 are affecting each other positively. Studies show that amount of Pitx 2 effect tooth growth. Besides, Pitx 2 also regulate of tooth orientation [111].

1.3.4.2. Other transcription factors

One of the HMG box family members that Lef 1 is a mediator of Wnt signaling pathway and its expression starts at the initiation stage through the end of the bell stage [112]. BMP4 regulate the expression of Lef 1 from the dental mesenchyme and again Lef1 regulate Fgf4 expression from enamel knot, which needed to Wnt signal to activation [42, 43]. Knockout

Lef 1 mice cannot develop teeth [79], but treatment of FGFs rescue the Lef1 mutant teeth [57].

The Cbfa 1/Runx 2 transcription factors are responsible of the osteogenic differentiation [112]. Mouse studies demonstrated that, expression of Cbfa 1/Runx 2 mRNA begins from the tooth mesenchyme at the early bud stage through the end of the cap stage. Cbfa1/Runx2 deficiency shows lack of teeth [113]. FGFs can induce Cbfa 1/Runx 2 expression in dental mesenchyme, but FGFs treatment cannot rescue the tooth of knockout Cbfa 1/Runx 2. Msx1 regulates the expression of Cbfa1/Runx2 [114, 115], while Msx1 also regulates Fgf3 expression from the dental mesenchyme [44]. So Msx 1 regulates Cbfa 1/Runx 2 expression controlling FGF 3 expression. All these transcription factors regulate the expression of growth factors that responsible for activation and regulation of other signaling molecules, in the developing tooth.

1.4. TISSUE ENGINEERING

Damaged tooth or loss of tooth is a common incident that effect human daily life. Traditional treatments for tooth repair may bring out material dependent problems that immune response by the patient system. Stem cell based tooth regeneration using tissue engineering techniques is a promising biological approach that aims to regenerate complete/tissue formation terms of histology, morphology and function [116]. Teeth organ development depends interaction between two main factors that dental epithelium and neural crest derived mesenchyme cells [24, 117]. Dental germ, pulp and deciduous teeth derived stem cells showed odontogenic ability in basic studies [118].

BMSCs are not ideal for implantation to old patients because these cells extremely lose their puripotency with increasing age [119]. However, studies with ASCs showed high rate of pluripotency with increasing age [120], and other different advantages over BMSCs. The main problem in tooth regeneration is to find appropriate scaffold and cell that can be compatible with body. Tooth organ engineering is complicated process; tooth stages needed to be defined and cell types must be well chosen. BMSCs and ASCs have multipotency that they can differentiate many of cells types especially osteocytes. Because of this ability they have under investigation in field of hard tissue engineering. But some difficulties of BMSCs

such as decreasing of multipotency by increasing donor age [120]. That's why; BMSCs cannot be appropriate for application of tooth engineering in the old humans. ASCs can maintain their multipotency with aging [121], which provide the high potential of treating damaged tooth via ASCs for hard tissue engineering [119]. ASCs have several advantages, they can differentiate into mesodermal origin cell types and also differentiate into nonmesodermal origin cell types including neurons, endocrine pancreatic cells, hepatocytes, endothelial cells, and cardiomyocytes [122]. Indicated that ASCs can effect repair of damaged organs, especially tooth. To form functional organ, scientists have proposed 'the functional tissue engineering' guidelines [123]. The following rules should be well designed and should be well evaluated for ASC application in the tissue engineering:

- Characterize functional achievements of the engineered tissue.
- Define *in vivo* biomechanical features of the tissue and determine biomechanical and metabolic requirements of the tissue to be replaced.
- Determine the bio- mechanical and physical features of the biomaterial scaffolds that can be used for tissue engineering.
- Designe well-matched engineered constructs of the biophysical microenvironment of the cells.
- Choose optimal inducers to regulate cell differentiation and tissue metabolism *in vitro* and *in vivo*.

Recent studies demonstrated that MSCs derived from in rats, dogs, and humans, have been transported to defective bone to repair sites in calcium phosphate porous ceramic scaffolds to form morphologically and biomechanically functional bone [124]. Likewise, MSCs used within hyaluronan and polymeric scaffolds for cartilage repair [125]. Another study showed MSCs have been seeded into the scaffolds *in vitro* and, implanted to host organism [126, 127]. Or this cell-scaffold composite was induced with differentiation medium to activate differentiation process into a specific lineage; after the induction structure was implanted

[128]. Other one, scaffolds are implanted to host and showed its effect without *in vitro* cell seeding but *in vivo* interaction [129]. All these techniques show well designed and characterized applications in the field of hard tissue engineering [130].

1.4.1. Scaffolds That Used in Hard Tissue Engineering

Extra Cellular Matrix (ECM) has great importance to tissue engineering field. However, variety of functions, complex structure and the dynamicity of ECM in native tissues make it hard to mimic. Hence, current modeling of scaffolding in tissue engineering should mimic the functions of native ECM. The main importance that played by scaffolds in engineered tissues are analogous to the functions of ECM in native tissues and are related with their structural, biological, and mechanical characteristics (Table 1.1).

Table 1.1 Main features of scaffold that used in tissue engineering [131].

Features of ECM in native tissue
Provides structural support for cells to reside
Contributes to the mechanical properties of tissues
Provides bioactive cues for cells to respond to their micro-environment
Acts as the reservoirs of growth factors and potentiates their actions
Provides a flexible physical environment to allow remodeling in tissue dynamic

1.4.1.1. Biodegradable Polymer Matrices

There are two types of biodegradable polymers:

- The natural materials
- The synthetic biodegradable polymers

The natural materials include polysaccharides (starch, alginate, chitin/chitosan, hyaluronic acid derivatives) or proteins (soy, collagen, fibrin gels, silk).

Synthetic polymers can be produced under controlled conditions and their features can be adjustable such as tensile strength, elastic modulus and degradation rate. This gives big advantage for producing step. These synthetic polymers have simple and well known structure. That's why, the possible toxicity, immunogenicity and favoring of infections are lower [132-135].

1.4.1.2. Saturated Aliphatic Polyesters

Saturated aliphatic polyesters are most preferred biodegradable polymers for 3D scaffolds. They are saturated poly- α -hydroxy esters, including poly lactic acid (PLA) and poly glycolic acid (PGA) and poly lactic-co-glycolide (PLGA) copolymers [136]. PLA can be forms: L-PLA (PLLA), D-PLA (PDLA), and DL-PLA (PDLLA).

Because of the chemical properties of these polymers, they can be go through the hydrolytic degradation by deesterification. PGA can be degraded to metabolites or eliminated by other mechanisms. Even though, PLA and PGA can be degraded easily, degradation products can cause an inflammatory response [137, 138]. Degradation rates of these polymers decrease in the following order: PGA>PDLLA>PLLA>PCL. Different factors may affect degradation of these polymers including; hydrophilicity, chemical compounds and structure, processing steps, molar mass, environmental conditions, crystallinity, porosity, distribution of chemically reactive compounds within the matrix [139, 140]. PLGA degradation rate was determined by composition of chains. Because of the absence of crystalline regions, PDLLA degrades faster. PGA gains hydrophobicity because of the methyl groups and this leads stronger acidity than PLA. Overall the initial degree of crystallinity of polymers affects the hydrolytic degradation [141].

To stabilize the pH and polymer degradation, several groups can incorporate with basic compounds, such as: bioactive glasses and calcium phosphates [139-141]. In other word, acidic compounds affect degradation rate. Recent studies have shown that, because of the

high mechanical stability, low molecular weight, biocompatibility and osteo stimulative features, PDLA has gained great interest as a drug carrier and scaffold material in tissue engineering field [142, 143]. Also, PCL was used as drug carrier for antibiotics, tissue engineering for bone growth and regeneration [144].

Table 1.2. Physical properties of synthetic, biocompatible, and biodegradable polymers used as scaffold materials [145].

Polymer	Melting Point T_m (°C)	Glass Transition Point T_m (°C)	Biodegradation Time (months)
<i>Bulk degradable polymers</i>			
PDLA	Amorphous	55-60	12-16
PLLA	173-178	60-65	>24
PGA	225-230	35-40	6-12
PLGA	Amorphous	45-55	Adjustable 1-12
PPF			Bulk
PCL	58.00	minus 72	>24
PHA	120-177	minus 2 to 4	Bulk
<i>Surface erodative polymers</i>			
Poly anhydrides	150-200		Surface
Poly ortho-esters	30-100		Surface
Poly phosphazene	minus 60 to 55	242.00	Surface

1.4.1.3. Polypropylene Fumarate (PPF)

PPF is unsaturated linear polyester and it is biocompatible that readily removed from the body by degradation. Degradation rate and time depends on molecular weight of PPF [135]. PPF was used in field of development of composite materials that combining with hydroxyapatite (HA) or bioactive glasses [146].

1.4.1.4. Poly-Hydroxy-Alkanoates (PHB, PHBV, P4HB, PHBHHx, PHO)

Poly-hydroxy-alkanoates (PHA) are aliphatic polyesters as well, but produced by microorganisms under unbalanced growth conditions [147, 148]. Semi-biodegradable features are making them usable as biomaterials. Last decade, poly-3-hydroxybutyrate (PHB), copolymers of 3-hydroxybutyrate and 3-hydroxyvalerate (PHBV), were shown to be usable for tissue engineering [132]. PHA polymers can be mixed with different polymers, enzymes or inorganic materials to arrange their biocompatibility and other features [132]. It was demonstrated that PHB can be used for bone tissue application [149]. Even though they are effective for hard tissue engineering, their restricted accessibility and the difficult and time consuming extraction procedure cause unwanted problems [150].

1.4.1.5. Surface Bioeroding Polymers

These polymers are poly-anhydrides, poly-ortho-esters and polyphosphazene. These polymers have been used in field of tissue engineering and drug-delivery. The surface bioeroding features provide several advantages over bulk degradation:

- Preservation of mechanical components which is mass to volume ratio, over the degradation process.
- Lower solubility leads minimal toxicity.
- Higher stimulative effect on bone growth into the porous scaffolds [151].

1.4.2. Bioactive Ceramics

Table 1.3. Mechanical features of bioactive ceramics [145]

Ceramics	Compressive Strength (MPa)	Tensile Strength (MPa)	Elastic Modulus (GPa)
Hydroxy Apatite	>400	~40	100
45S5 Bioglass	~500	42	35
Glass-Ceramic A/W	1080	215	118
Porous bioactive glass 70S30C 82 %	2.25		
Porous Bioglass derived glass ceramic >90 %	0.2-0.4		
Porous Hydroxy Apatite 82-86 %	0.21-0.41		$0.83-1.6 \times 10^{-3}$
Cortical Bone	130-180	50-151	12~18
Cancellous Bone	4~12		0.1-0.5

1.4.2.1. Bioactive Glasses and Glass-Ceramics

Scientist demonstrated that some glass compositions showed great biocompatibility at *in vivo* bone regeneration [152]. Bioactive glasses chemically bind to host bone and this is known as bioactivity that interaction with carbonated hydroxyapatite (HCA) sheet on the glass surface when implanted [152-154]. Studies with HA and calcium phosphates show an excellent ability to interact with bone. Addition to this, in tissue engineering, bioactive glasses can stimulate enzyme activity, vascularization, foster osteoblast adhesion, growth, differentiation; and induce the differentiation of mesenchymal cells into osteoblasts [155-160].

Recent studies proved that 45S5 Bioglasss composition, upregulate the gene expression that control osteogenesis and the production of growth factors [161]. Also, combination with HA and 45S5 Bioglasss leads bone growth and it has higher osteo inductivity than pure HA [162]. That's why; 4S5S Bioglass was preferred as scaffold material in tooth and bone regeneration [152].

1.4.2.2. HA and Calcium Phosphates

Around 60 wt% of bone and enamel are made of HA which is intensively investigated as the main part of scaffold materials for hard tissue engineering [163]. Due to their similar chemical and crystal structure with tooth and bone minerals, calcium phosphates have a great biocompatibility [164]. *In vivo* and *in vitro* studies were proved that, all forms and phases of calcium phosphate induce the attachment, differentiation, and proliferation of stem cells, and HA is the most effective one among them.

Mechanical properties of tooth change, because of its crystallinity, porosity, and composition, at the development of body. These mechanical properties of synthetic HA and developing tooth have shown significant similarities. HA is representing great inductive material for hard tissue engineering. Hence, calcium phosphates alone cannot be used for scaffolds material even though its biocompatibility and osteoconductivity.

2. AIM OF THE STUDY

Hard tissue scaffolding with certain cell types for mimicking immature tooth at the late bell stage can be difficult to obtain all necessary structures include dentin, ligament, enamel, pulp and cementum. Even though mechanical and biological effects of HA for the body was known, harmony of BMSCs, neural crest derivative ADSCs and ectoderm derivative epithelium in HA were unidentified. Previous studies have shown that, forming functional tooth; enamel, dentin and pulp components must be molded to obtain fully grown tooth. Meanwhile, developmental stages of tooth should be created via creating dentin, ligament, enamel, pulp and cementum. This study aimed to regenerate functional tooth by mimicking late bell stage in *in vitro* conditions, with qualitative and quantitative examinations.

- Epithelium was seeded in collagen coated porous tooth shaped HA scaffold,
- Differentiated neural crest derivative ADSCs were mixed with Matrigel and seeded in HA scaffold,
- Last structure was coated with BMSCs.

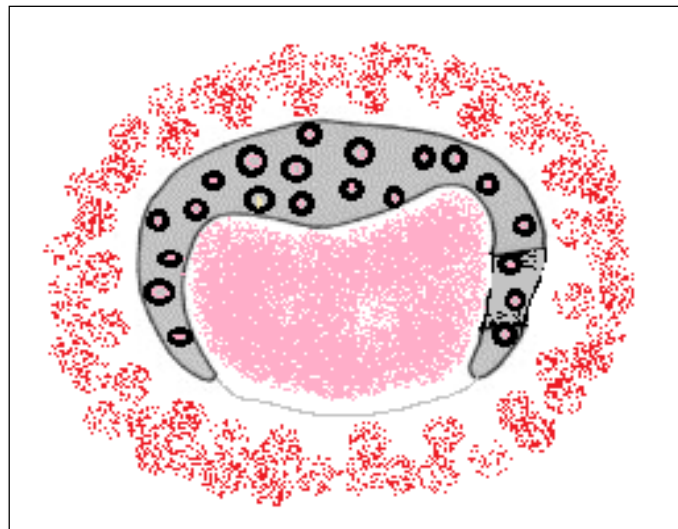


Figure 2.1. *In vitro* tooth shaped construct demonstration.

3. METHOD

3.1. SCAFFOLD CHARACTERIZATION

3.1.1. Preparation of Tooth-shaped Scaffolds and Cell Seeding

The scaffolds were prepared using Agarose with HA. It is a new method that integrates the gel-casting and salt dissolving methods. 7% (w/v) Agarose in dH₂O and 40% (w/v) HA were boiled. Before the polymerization by cooling, 50% (w/v) ~300 μ m NaCl was added and mixed with HA slurry. After the polymerization the NaCl in the construct was dissolving in dH₂O for 24 hours. After the dissolving process, the constructs were dried in air for 24 h. Constructs were prepared in the shape of human molars at late bell stage. Tooth shaped scaffolds were coated with collagen overnight at 4°C, washed in DMEM, and seeded with 2 x 10⁶ cells in DMEM for 1 hour at 4°C.

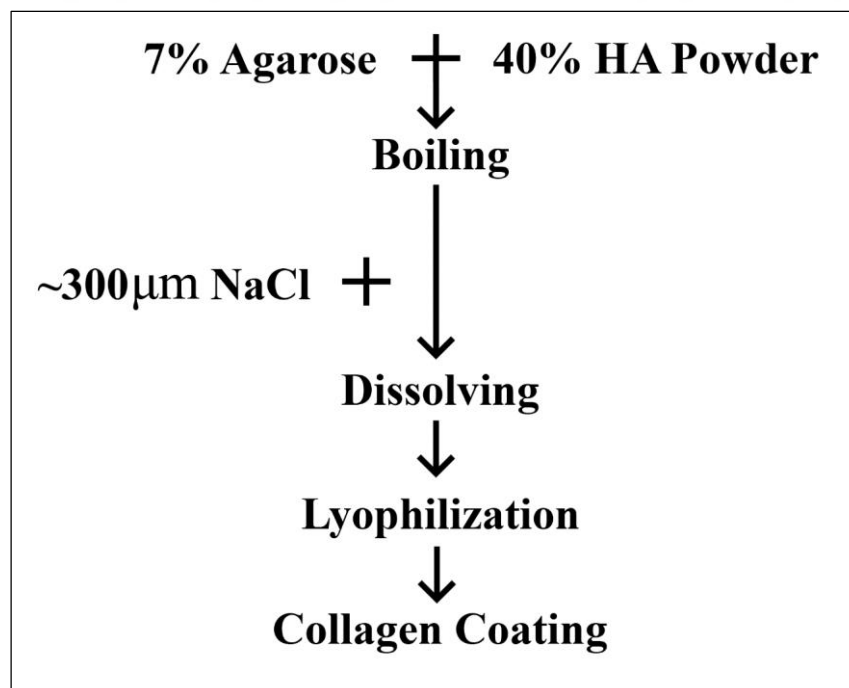


Figure 3.1. A flow chart of process steps for scaffold fabrication using combined Agarose and NaCl methods.

3.1.2. SEM

SEM analysis was used to determine the porosity and interconnectivity of the HA scaffolds with and without human ADSCs. The cell seeded on scaffold and treated with proper fixative including; 3% glutaraldehyde, 0.1 M sodium cacodylate and 0.1 M sucrose for 1 hour, and dehydrated with alcohol dilutions. Scaffolds were placed into holders and covered with coated gold with sputter coater (BAL-TEC SCD 005, Switzerland). SEM images were evaluated by using SEM Zeiss EVO 40 (Jena, Germany).

3.1.3. Porosity and Density Measurements

A liquid replacement technique was used to evaluate the porosity and density of HA scaffolds. The density measurements obtained data about pore size and distribution, permeability, and presence of physical abnormalities in HA hybrid scaffold. A scaffold of weight (W) was immersed in a graduated cylinder containing a certain volume (V1) of ethanol (EtOH). The cylinder was placed in vacuum to force the EtOH into the pores of the scaffold until no air bubble exit from the scaffold. The total amount of the EtOH and HA scaffold was then measured as V2: The volume difference (V2 - V1) was the volume of the skeleton of the HA scaffold. The scaffold was removed from the EtOH and the residual EtOH volume was measured as V3: The total amount of the scaffold, V; was then

$$V = V2 - V3.$$

The measured density of the scaffold, ρ was calculated as

$$\rho = W/(V2 - V3)$$

The porosity of the open pores in the scaffold, m was measured as

$$e = (V1 - V3)/(V2 - V3)$$

3.1.4. IR Spectroscopy

IR was used to characterize HA powder before and after scaffolding process. Polarized fourier transformed infrared (FTIR) spectra of ATR with a depth of penetration of over 2 microns at 1000 cm^{-1} were obtained using a Thermo Scientific Nicolet™ iS™ 10 FTIR

spectrometer with a Attenuated Total Reflectance (ATR) sampling accessory and a solid transmission sample compartment. Spectrum analyses were performed using standard Nicolet iZ10 and Omnic software. FTIR spectra were taken on both HA nano powder and HA scaffold.

3.2. CELL CHARACTERIZATION AND SEEDING

3.2.1. Isolation and Characterization of hBMSCs, hASCs and Epitelial Cells

Minced Adipose tissue was digested in 3% Collagenase II for 30 minutes at room temperature. After the digestion process santrifugation was performed at 500 g for 10 minutes. Pellet was seeded on tissue culture flasks (BIOFIL, TCP, Switzerland) and when cells cover the 80 % of flask in Dulbecco's Modified Eagle's Medium (DMEM) supplemented with 10 % (v/v) fetal bovine serum (FBS) and 1% (v/v) PSA (10.000 units/mL penicillin, 10.000 µg/mL streptomycin, 25 µg/mL amphotericin B) (Invitrogen, Gibco, UK) [165].

Human bone marrow and gingival epithelium were collected from the mandibular bone and gingival tissues around 3rd molar tooth. The collected bone marrow from jaw bone was harvested and characterized for the MSCs surface markers by flow cytometry.

Bone marrow was collected from the mandibular bone, following Yeditepe University Ethical Commitee approval. The collected bone marrow from jaw bone was harvested. The bone marrow tissue was plated in six well plates (BIOFIL, TCP, Switzerland) and grown to confluency in DMEM supplemented with 10% (v/v) FBS and 1% (v/v) PSA (10.000 units/mL penicillin, 10.000 µg/mL streptomycin, 25 µg/mL amphotericin B) (Invitrogen, Gibco, UK). The harvested cells expanded and started to appear after 3-4 days, and covered the surface after 8 days. Thereafter, the cells were trypsinized using 0.25% (v/v) trypsin/EDTA (Invitrogen, Gibco, UK). Medium was added to detached cells to inhibit the activity of trypsin. After the cells were centrifuged at 300 x g for 5 minutes at room temperature, the pellet was dissolved in fresh medium and seeded on a T-75 flask (Zelkultur

Flaschen, Switzerland). The cells were maintained at 37°C and 5% CO₂ in a humidified incubator. Cells from passages 3~4 were used in all experiments.

ASCs and BMSCs were characterized by using antibodies against CD29, CD14, CD31, CD34, CD44, CD45, CD90, CD105, CD73 and Integrin.

Human epithelial tissues were digested by incubating tooth roots at 37°C for 1 hr in 50 mL with PBS containing 0.67 mg/mL of collagenase type II and 0.3 mg/mL of dispase. Second digestion was performed with 2.0 mg/mL collagenase type I, and 0.25% trypsin for 1.5 hours at 37°C in DMEM. After the digestions steps, cells were filtered through a 40 µm cell strainer re-suspended in DMEM including FBS and PSA and placed in culture conditions.

3.2.2. *In Vitro* Odontogenic Induction

Odontogenic differentiation medium was prepared by conditioning the culture medium with 50 µg/mL ascorbic acid, 50 nM β-glycerol phosphate, and 10⁻⁸ M dexamethasone (DXM), cells were treated with this medium on every other day for 14 days. Control groups; one of them was treated with odontogenic medium only as a positive control, other one was added nothing as a negative control.

3.2.2.1. *Alkaline Phosphatase Activity (ALP)*

After the process of odontogenic induction, ALP activity of the cells was determined. Medium was removed from the wells, and 0.2% (w/v) Triton-X-100 was added to cells for lysis. Cells were harvested from 6 well plates and mixed by vortexing for 20 minutes at room temperature. 10 µl of lysate was added to each well of 96 well plates, and then 90 µl of ALP solution was added to lysates by multichannel pipette. Absorbance was measured by ELISA plate reader to determine ALP activity.

3.2.2.2. *Alizarin Red Staining*

Alizarin Red assay is based on evaluation of the free calcium or calcium deposits. Cells were seeded on 6 well plates at a concentration of 50.000 cells/well. Cells were fixed by 500 μ l of paraformaldehyde for 20 minutes and rinsed with PBS for 3 times. After addition of 3% (w/v) silver nitrate, the cells were incubated under UV light for 1 hour at room temperature. Cells were rinsed with PBS for 3 times and 5% (w/v) sodium thiosulfate was added into each wells following an incubation for 2 minutes at room temperature. Cells were observed under the light microscope.

3.2.2.3. *Quantitative Real Time Polymerase Chain Reaction*

Total RNA isolation was completed using the High Pure RNA isolation kit according to the manufacturer's instructions. RNA samples were translated into cDNAs with High Fidelity cDNA synthesis kit. Gene levels were evaluated by Real Time PCR using Maxima SYBR Green kit. cDNA synthesized were used as a template for gene level analysis. Ododntogenesis Related Genes: *BMP4*, *COL1A*, *DSPP* and as a housekeeping gene *GAPDH* was used.

Table 3.1. RT-PCR reagents

Sybr Green 2X	10 μ L
Forward Primer	1 μ L
Reverse Primer	1 μ L
dH ² O	4 μ L
Template (100ng/ μ L)	4 μ L
Total Volume	20 μ L

Table 3.2. RT-PCR conditions

Cycle	Repeat	Step	Dwell Time	Set Point
1	1	1	5 minutes	95°C
2	40	1	30 seconds	95°C
-	-	2	40 seconds	58°C
-	-	3	50 seconds	72°C
3	1	1	10 minutes	72°C
4	110	1	12 seconds	40°C
5	1	1	-	4°C

3.2.3. ELISA

Levels of FGF 3, FGF 10 and BMP 4 were measured by enzyme-linked immunoassays (OptEIA ELISA, BD Biosciences, Lille, France for HGF) in supernatants of cell seeded on tooth shaped scaffold culture.

3.2.4. Histopathology

After 8 weeks, developing tooth scaffolds were excised, fixed in 4% formalin, embedded in paraffin and thin-sectioned. 0th, 4th, and 8th week samples were collected and stained. Analyses included: Hematoxylin and Eosin Y (H&E) and Tricrome Masson stainings. Tricrome Masson staining was performed with following procedure; Sections were deparaffinized with incubation at 65°C and they were treated with xylene and EtOH dilutions to bring water. Sections were rinsed with distilled H₂O and placed into solution A (Acid Fucsin, dH₂O and Glacial Acetic Acid) for 10 minutes and rinsed with tap water. Sections were placed into solution B (Phosphomolybdic Acid and dH₂O) for 5 minutes and rinsed with tap water. Sections were placed into solution C (Methyl Blue, Glacial Acetic Acid and dH₂O) for 10 minutes and rinsed well with dH₂O. Dehydration processed with EtOH and cleared with xylene. H&E staining was performed with following procedure; Sections were deparaffinized with incubation at 65°C and they were treated with xylene and EtOH dilutions to bring water. Sections were rinsed with dH₂O and placed into solution Hematoxylen for

3,5 minutes and rinsed twice with water. Sections were placed into solution 1 % of Acid Alcohol for 1 minute and rinsed with water. Sections were placed into ammoniac solution for 0,1 second and rinsed with water. Sections were placed into 96 % EtOH solution for 30 seconds and placed into Eosin Y solution for 6 minutes. Dehydration processed with increased EtOH dilutions and cleared with xylene.

3.2.5. Immuno-histochemical Analysis

Immunohistochemical analysis was performed to determine cell morphologies and immature tooth at the late bell stage with bone morphogenic protein 2, 4, 7 (BMP 2, 4, 7), amelogenin, collagen type 1 (COL1A), dentin matrix protein 1 (DMP 1), dentin sialo phosphoprotein (DSPP), vascular endothelial growth factor (VEGF), CD 31 and Msx 1. Immunohistochemical staining to tooth shaped scaffold at the 0th 4th and 8th weeks were performed on paraffin sections.

3.2.6. Statistical Analysis

All graphics were prepared using the Microsoft Office Excel and GraphPad Prism5 softwares. Standard errors and t-test values were calculated using GraphPad Prism5 software. For statistical analysis student t test was used in the GraphPad prism5 programs. P value less than 0.05 was considered as statistically significant.

4. RESULTS

4.1. CELL ISOLATION AND CHARACTERIZATION

4.1.1. Isolation and Characterization of Gingival Epithelial Cells (GECs)

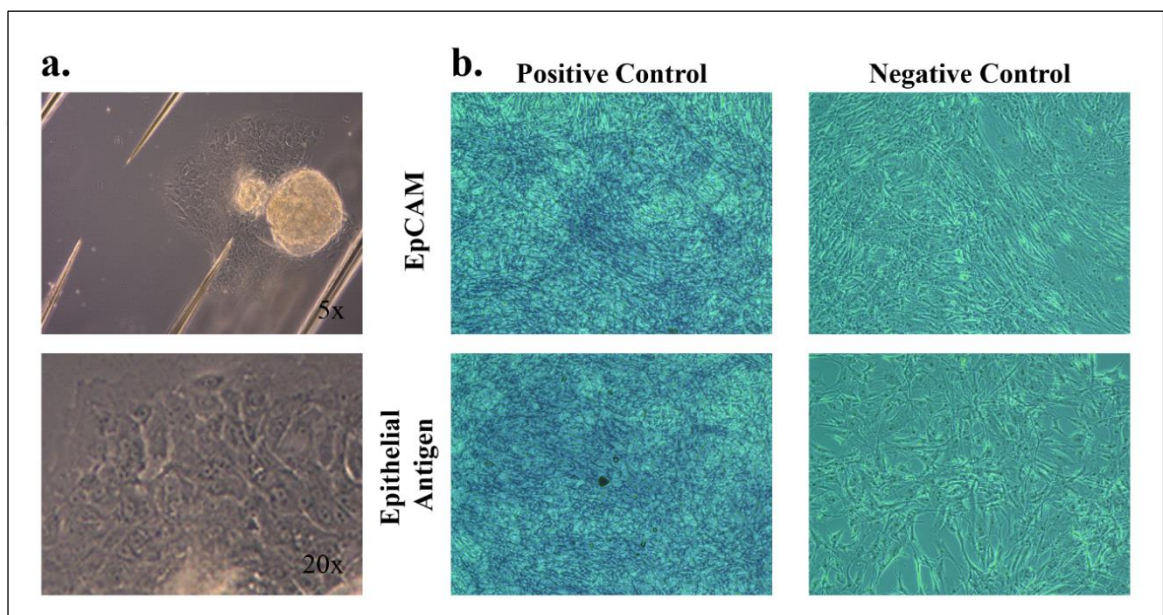


Figure 4.1. a. Primary gingival epithelial cell light microscope images (5x, 20x). b. Epithelial cell specific antibody staining (EpCAM, Epithelial Antigen) (5x).

Gingival tissue was collected from the gingiva and third molar tooth germ, following Yeditepe University Etik Kurulu approval. Briefly, gingival tissue was obtained from a healthy gingival tissue. Following rinsing in Ca-Mg free Phosphate Buffered Saline (PBS) containing 1 % of Streptomycin, Penicillin and Amphotericin, tissue were incubated overnight in 0.4 % dispase at 4°C. Epithelial layers were then mechanically disattached and trypsinized for 10–15 min at 37°C in 0.05 % trypsin-0.53 mM EDTA. After pipetting, the cell suspension was centrifuged for 5 minutes at 700 g and the cell pellet resuspended in HuMEC Ready Medium (Basal Medium; Thermo Scientific, Pittsburg, PA, USA). Cells

were cultured at 37°C, 5% CO₂, with humidity, and used for assays between passages 3 and 5.

4.1.2. ASCs isolation and Characterization

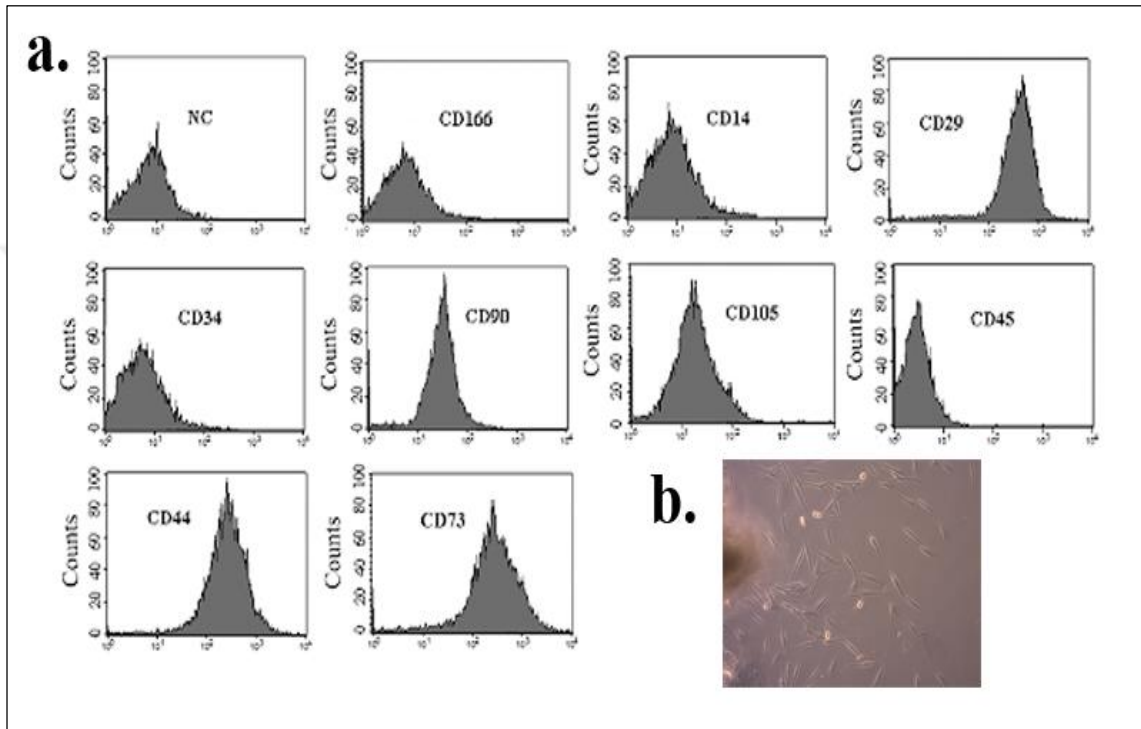


Figure 4.2. Characterization of fat derivative stem cells. a. Adipose stem cell image. 10X.
b. Stem cell characterization of cell derived from fat tissue.

Adipose tissue was collected from the lipoaspirated fat, following Yeditepe University Etik Kurulu approval. The process is summarized in Figure 5. In brief, the lipoaspirated tissue was washed. The upper part containing adipose tissue is digested with collagenase for 1 hour and centrifuged at 400 g. After centrifugation, the pellet is known as the SVF which was obtained large yields about 2×10^4 cells per 1 mL. Cells within the SVF subsequently attached to poly L-lysine coated tissue culture flasks under standard incubation conditions.

4.1.2.1. Odontogenic Differentiation of hASCs

Characterized hASCs were seeded on plate for odontogenic induction for 2 weeks. Calcium deposits were evaluated by Alizarin Red staining. Figure 4.3.a shows Ca deposits on differentiated cells (left), negative control shows any Ca deposition and odontogenic induction (right). Alkaline phosphatase activity measurements was performed to calculate differentiation levels (Figure 4.3.b). *COL1A* and *DSPP* gene levels were measured by RT-PCR. These genes play important role of hard tissueformation and dentinogenesis (Figure 4.3.c). All mesurement show that odontogenic induction was done successfully.

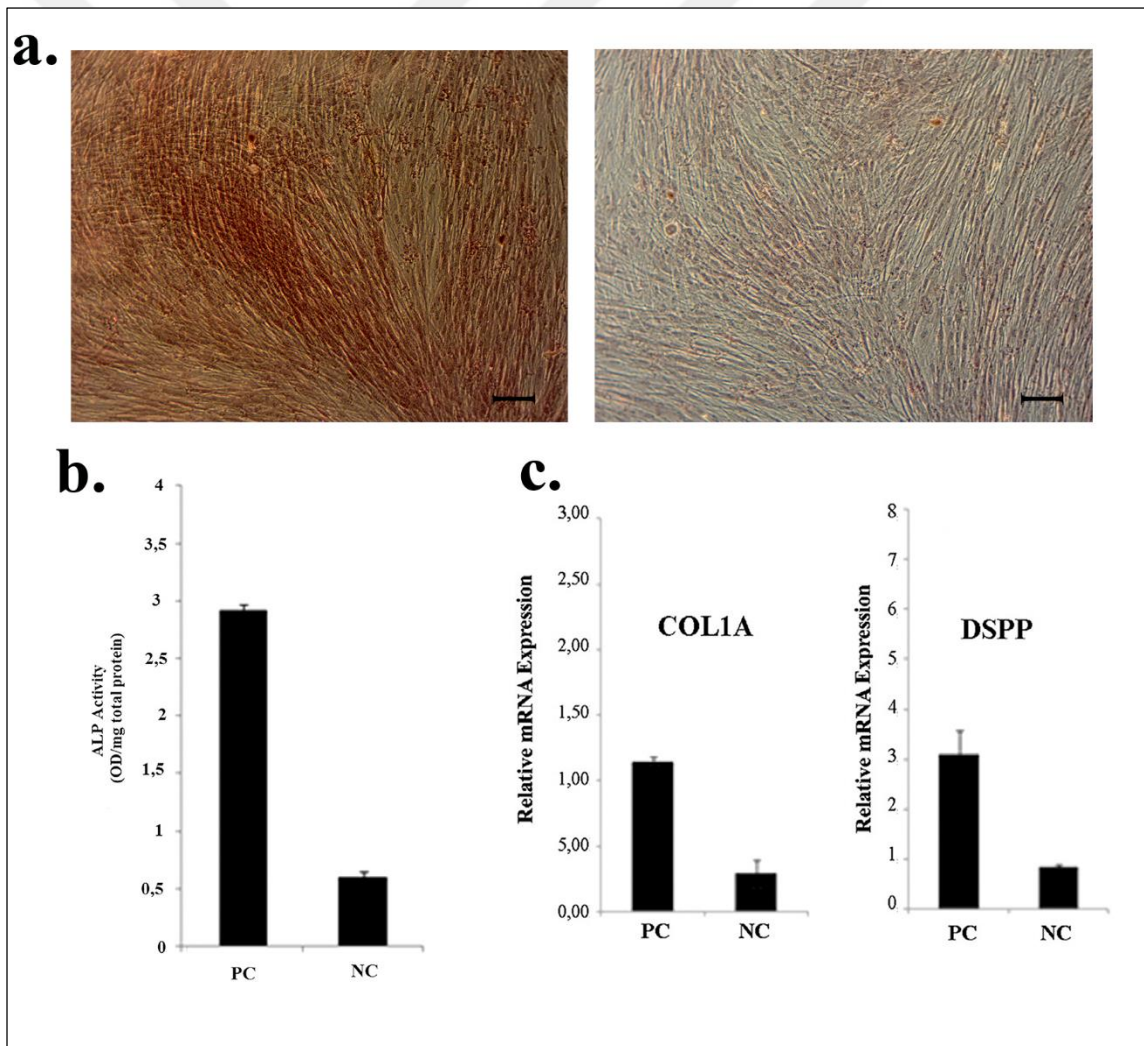


Figure 4.3. Odontogenic differentiation of hASCs. (a) Alizarin Red Staining, (b) Alkaline Phosphatase (ALP) Activity of cells, (c) Real-time polymerase chain reaction analysis: relative messenger RNA expression of *COL1A* and dentin sialophosphoprotein (*DSPP*), NC, nontreated cells; PC, odontogenic medium only. Scale bars = 100 μ m.

4.1.3. BMSCs Isolation and Characterization

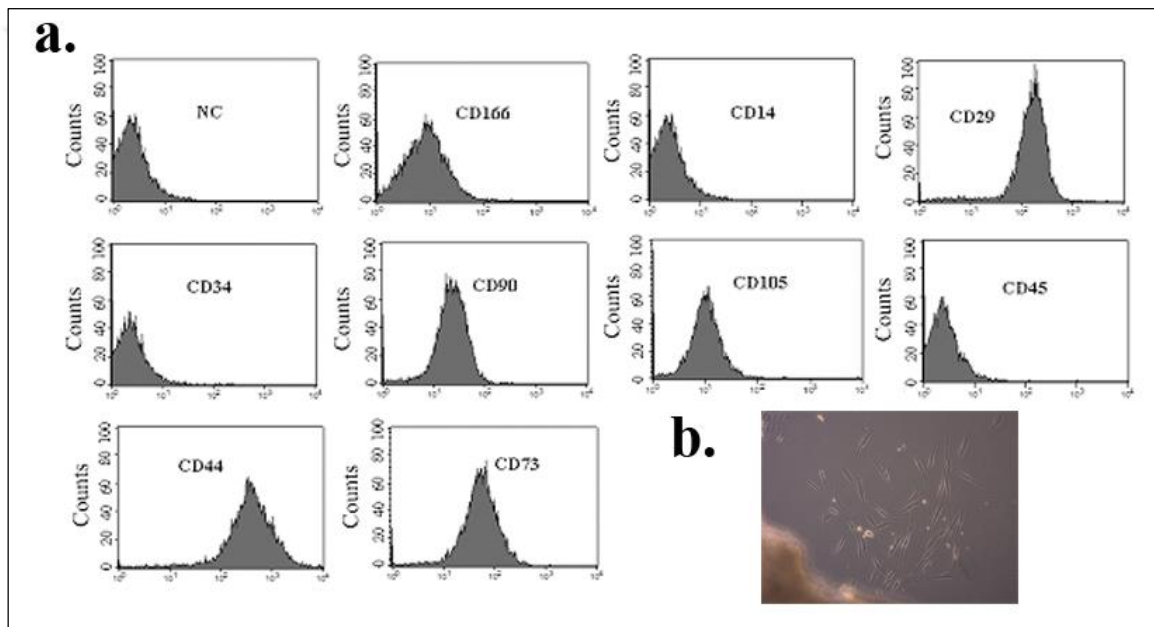


Figure 4.4. a. Stem cells from jaw bone marrow. 10X. b. Human bone marrow stem cell characterization, isolated from mandibular bone.

4.2. SCAFFOLD CHARACTERIZATION

4.2.1. Porosity and density measurements

The obtained density of a porous scaffold can influence its physical strength, permeability, and presence of structural defects. Table 4.1 shows the density and porosity of HA scaffolds prepared with mixture of different HA concentrations. Porosity characterization is based on the presence of open pores which are related to possessions such as permeability and surface area of the porous structure. High porosity usually means a high surface area/volume ratio, and thus favors cell attachment to the related scaffold and altered hard tissue regeneration. Table 4.1 shows that scaffolds with approximately the same porosity but higher HA concentration have higher density. As the HA concentration was increased, the pores turn into interconnected with more dense and thicker pore walls, important factors that improve the mechanical properties of the porous scaffold. It is useful stating that for a fixed HA concentration,

Table 4.1. Density and porosity values at changing HA concentrations

HA Concentration	Pore Size	Density g/cm³	Porosity %
35 % (wt/vol)	150-300 μm	0,043 \pm 0,002	84,2 \pm 0,3
40 % (wt/vol)	150-300 μm	0,048 \pm 0,002	91,5 \pm 0,3
45 % (wt/vol)	150-300 μm	0,051 \pm 0,002	90 \pm 0,3
50 % (wt/vol)	150-300 μm	0,055 \pm 0,002	87,1 \pm 0,3

4.2.2. SEM Images of Scaffold with and without cells

The scaffolds should exert to the tooth characteristics not only in terms of composition but also in terms of pore physiology. Porous scaffolds allow development of tooth and soft tissues within large pores and also blood supply for further hard tissue mineralization.

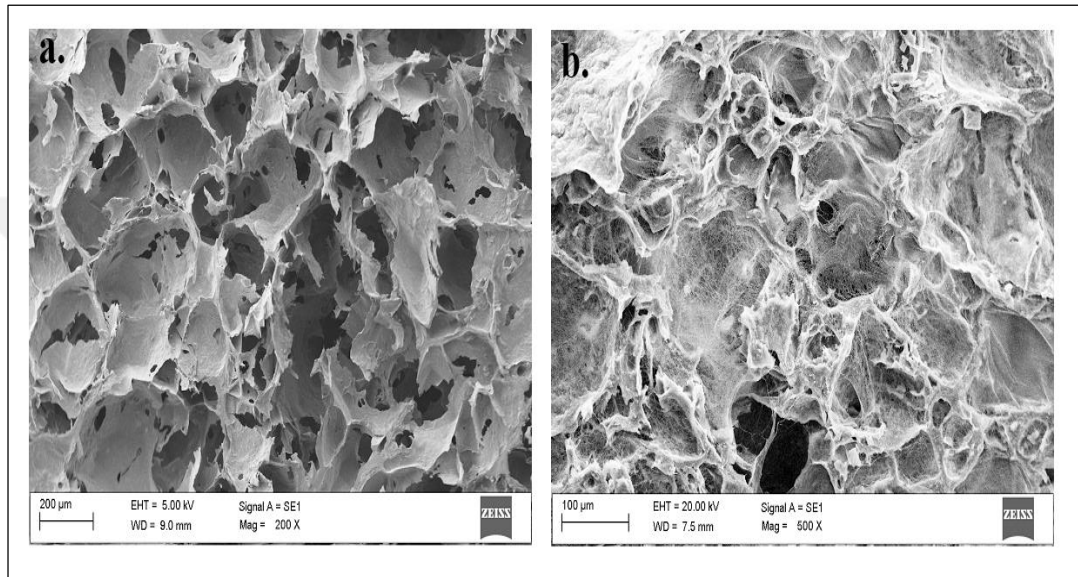


Figure 4.5. SEM images show the porous structure of HA hybrid scaffold with open and connective form. SEM images of interconnected porous of HA scaffold prepared with mixture containing 40 wt % HA (b) with and (a) without cells.

SEM images in Figure 4.5. show the interconnected, macroporous structures of the scaffolds with (Figure 4.5.b.) and without (Figure 4.5.a.) cells, prepared with HA mixtures. Scaffolds of different pore sizes ranging from 100 to 300 µm were prepared in this study. All samples showed basic structural characteristics of a continuous open structure, with a 3D interpenetrating network of struts and pores. Hulbert et al. suggested that the optimum pore size for osteoconduction is 150-200 µm.

4.2.3. FTIR

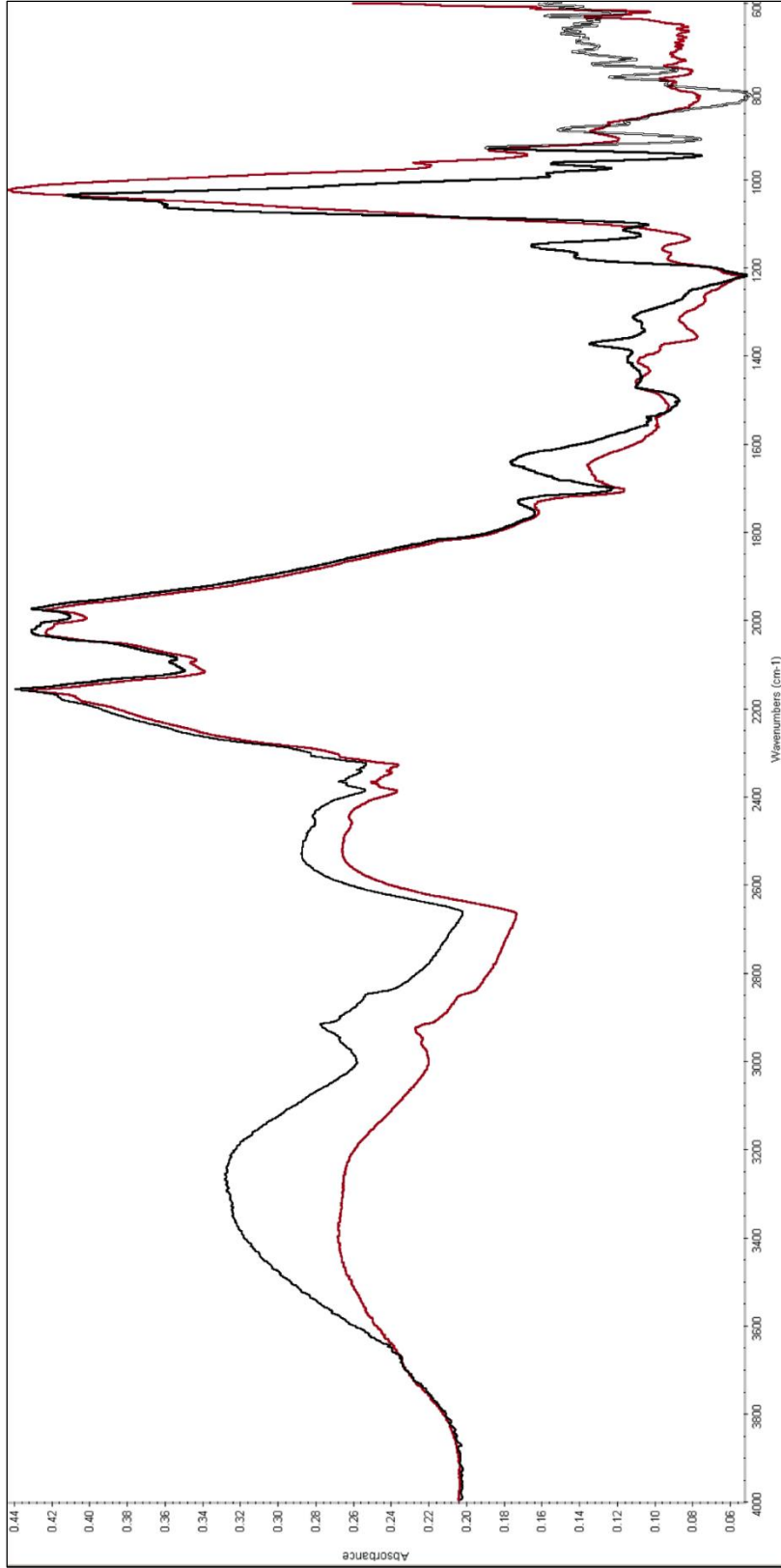


Figure 4.6. FTIR spectra of HA scaffolds. Figure shows difference between (black line) HA powder and (red line) scaffolded HA.

In the IR spectra, two lines at 630 and 3570 cm^{-1} correspond to the vibration of OH ions, 1030 and 570 cm^{-1} are the typical lines of phosphate bending vibration, while the line at 985 cm^{-1} is known to phosphate stretching vibration. The lines at 881, 1420 and 1460 cm^{-1} are indicative of the carbonate ion substitution. The lines at 1650 and 3470 cm^{-1} correspond to H_2O absorption. The analyses of these bands confirmed that the spectra shown in Figure 4.6 belong to HA [46,47]. There wasn't any noticeable spectrum difference between the HA powder and HA scaffold, which further confirms that no chemical decomposition occurred during the HA scaffolding process.

4.2.4. Alizarin Red Staining of Scaffolds

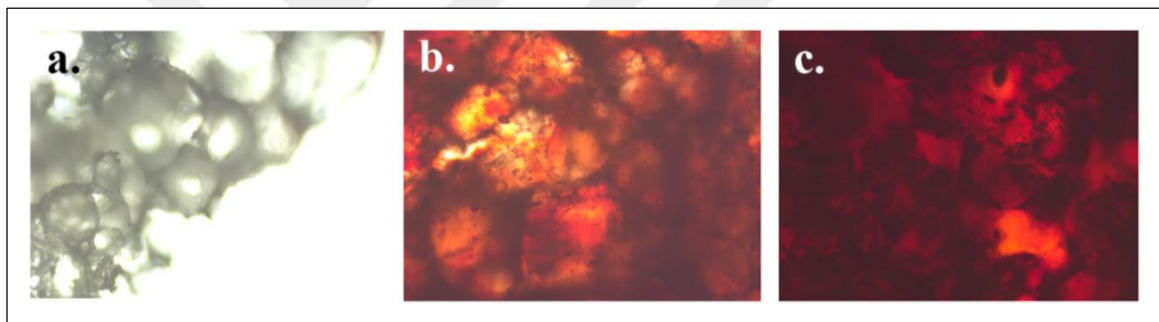


Figure 4.6. Light Microscopy image of interconnected porous HA scaffold prepared with slurries containing 40 wt% HA (a) 200X, image of HA scaffold stained with (c) Alizarin Red Stain with and without (b) odontogenically differentiated cells.

4.3. TOOTH CONSTRUCTION WITH HA HYBRID SCAFFOLD

4.3.1. ELISA

Cells were seeded on HA porous scaffold and treated with odontogenic media for 8 weeks. Media was collected every week to measure secreted cytokines and growth hormones. Figure 4.8 shows FGF 3, FGF 10 and BMP 4 release from differentiated construct which are related

with dentinogenesis. FGF3 and FGF10 expressed from dental mesenchyme at the bud stage. While FGF10 can stimulate cell proliferation only in the epithelium but not in the mesenchyme, FGF3 can stimulate cell proliferation in isolated mesenchyme [47]. BMP 4 expressed from enamel knot, may be cause for apoptosis in the knot cells at the end of the late bell stage and started to express dental mesenchyme.

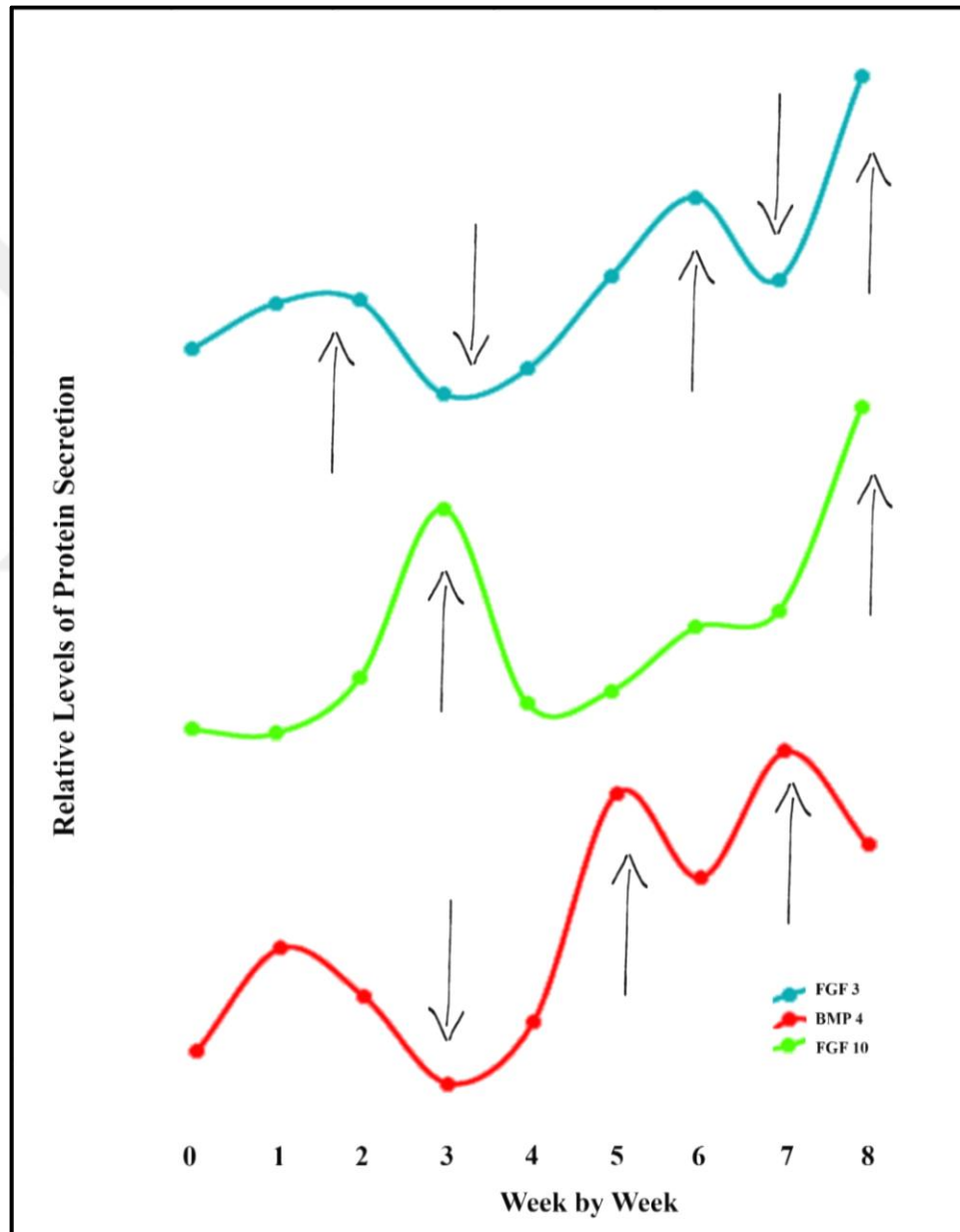


Figure 4.8. Relative FGF 3, FGF 10 and BMP 4 proteins release from cells seeded on tooth shaped scaffolds for 8 weeks.

Secretion profile of FGF 3 and FGF 10 in first weeks not parallel, this shows cross-talk between epithelial and mesenchyme cells. Firstly, at the 3rd week FGF 10 expression started to increase to proliferate epithelial cells to form enamel knot. Meanwhile FGF 3 and BMP 4 release were started to decrease. At the 4th week, forming enamel knot were secreted BMP 4 to trigger to dental mesenchyme proliferation, differentiation and differentiation. And also at the 7th week enamel knot was started to release FGF 3 to alter dental mesenchyme to start dentinogenesis. At last week cells were differentiated and the cells started to form dentin and enamel.

4.3.2. Histopathology

H&E staining of tooth construct at the 0th, 4th and 8th week (Figure 4.9., 4.10. and 4.11.). At the 0th week disoriented cells can be seen on scaffold (Figure 4.9.a, b, d) or mesenchymal derivative odontoblastic cells (Figure 4.9.a, c, d). Also non degraded porous structure can be seen at Figure 4.9.d.

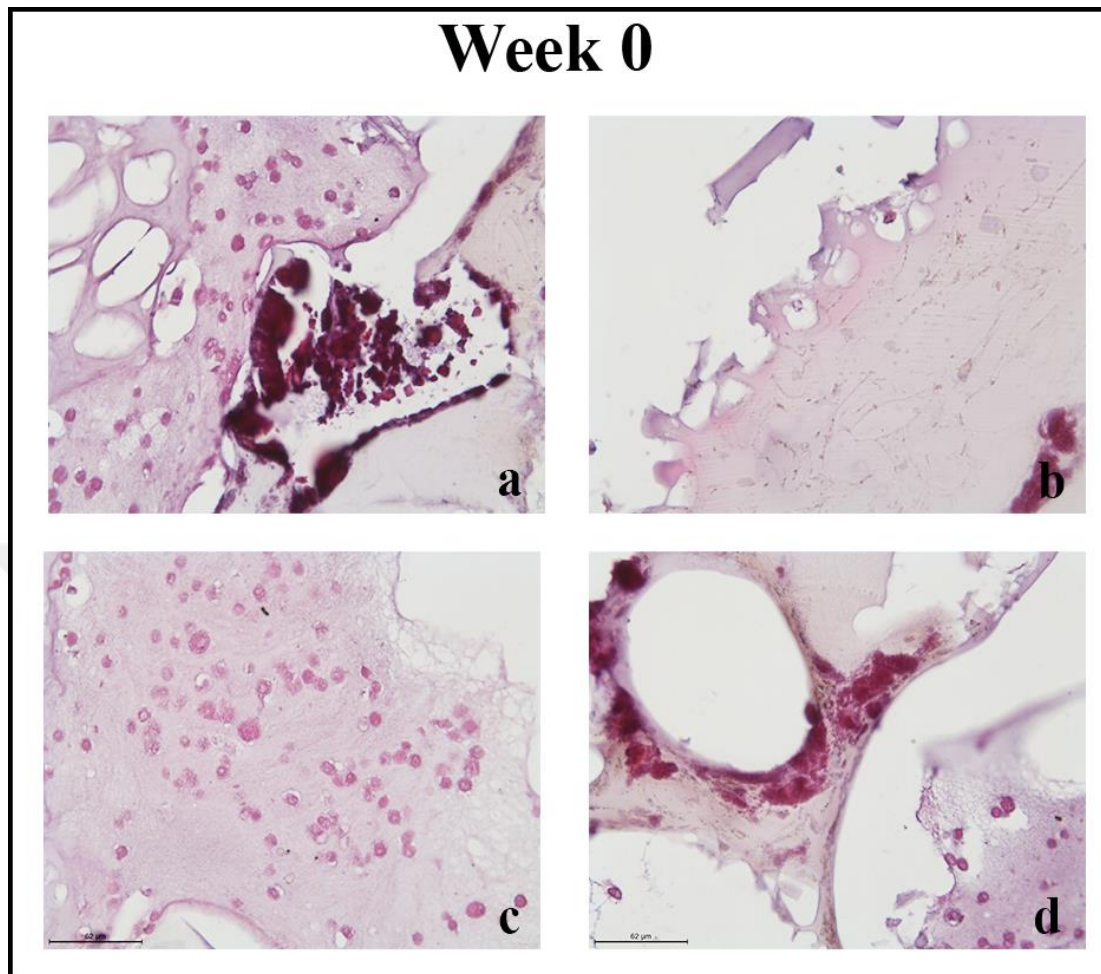


Figure 4.9. H&E staining of 0th week tooth shaped grafts

At the 4th week cells started to localized and differentiated and also scaffold started to degrade by cells. Moreover, predentin (Figure 4.10.a), low level of dentin (Figure 4.10.b) differentiated odontoblasts (Figure 4.10.c) and pulpa matrix formation (Figure 4.10.d) were started to form.

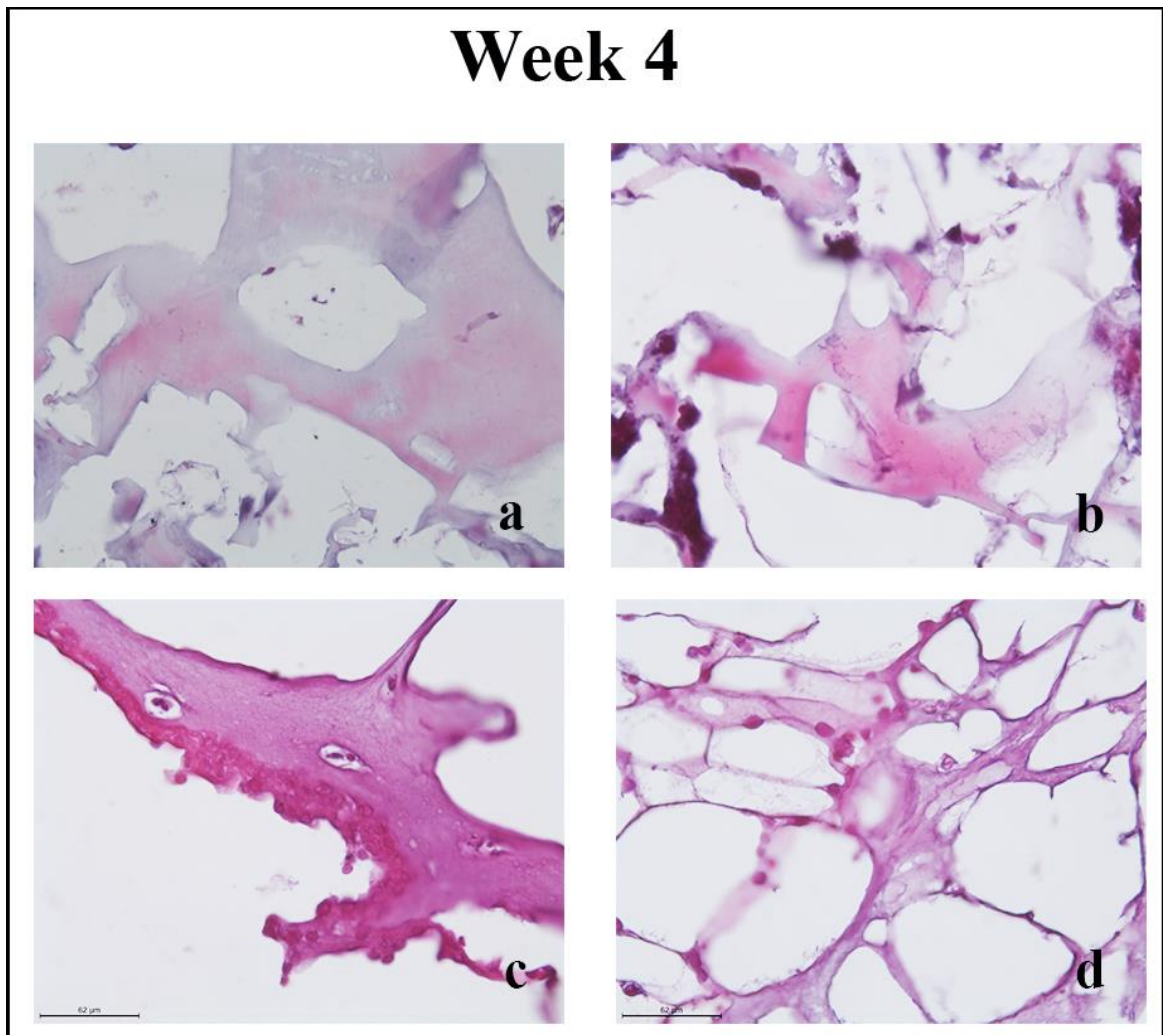


Figure 4.10. H&E staining of 4th week tooth shaped grafts

At the 8th week mature cells and structures are seen such as cementoblastic cell forming into outer mesenchymal part (Figure 4.11.a), differentiated epithelial and odontoblasts are communicate and express dentin and enamel precursors (Figure 4.11.b), mature dentin formation trigger thr epithelial cells to enamel formation (Figure 4.11.c) and differentiated and specialized epithel rests of malasses appers (Figure 4.11.d).

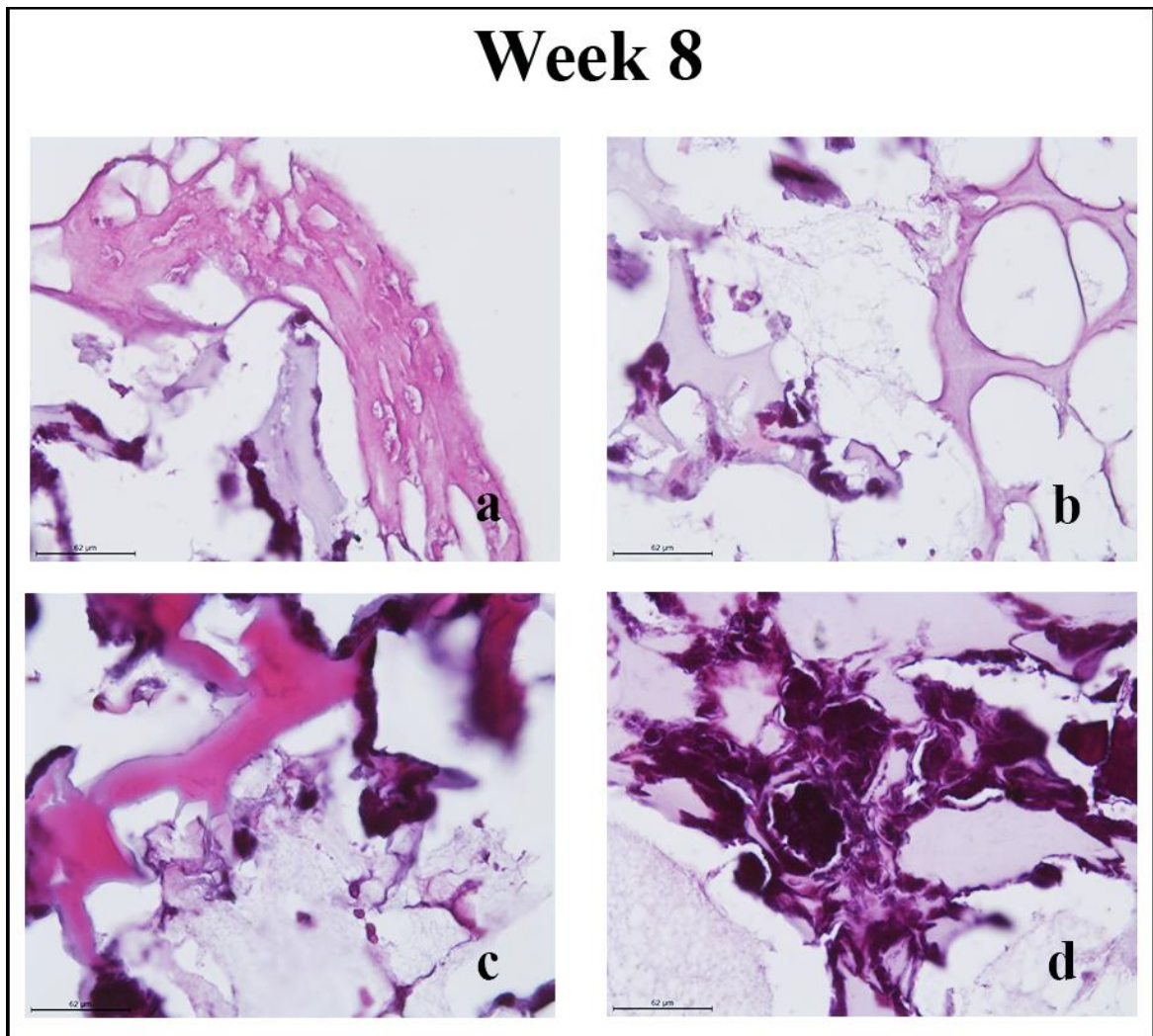


Figure 4.11. H&E staining of 8th week tooth shaped grafts

Tricrome masson stained parts show collagen secreted parts. Collagen secretion mainly occurs pulp section (Figure 4.12.a, b) and odontoblast cells (Figure 4.12.b,c)

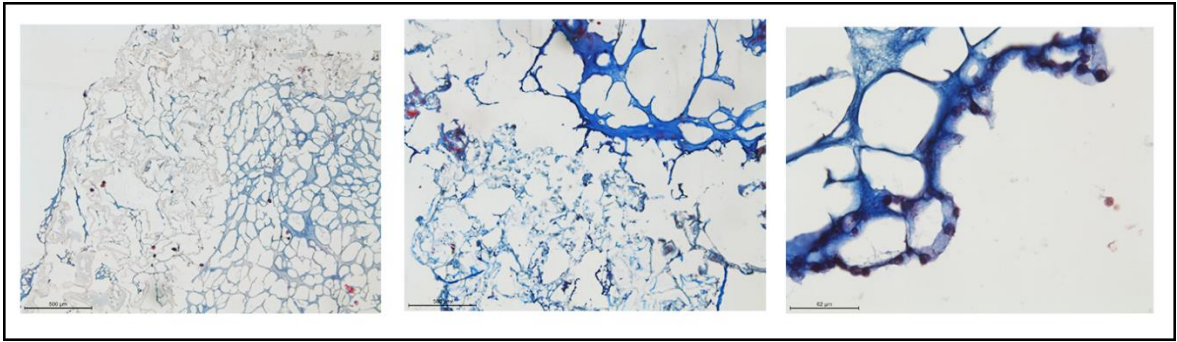


Figure 4.12. Tricrome Masson staining of 8th week tooth shaped grafts

Figure 4.13 shows specialized structures for tooth development. Firstly, the cells were forming cementocytes like morphologies (Figure 4.13.a) and also cementoblast are started to form in to outer mesenchymal part (bone marrow stem cells) (Figure 4.13.b).

In Figure 4.13.c dentinogenesis were started. Purple parts indicate epithelial cells and opposite site surrounded by odontoblasts, pink regions indicate dentin. After the 4th week enamel knot started to appear Figure 4.13.d.

Enamel knot are created by spetialized epithelial cells which play important role on tooth growth untik mineralization. Figure 4.13.e shows differentiation of epithelial cells which are started to form long shaped morphology to communicate with dentin forming odontobalsts and started to enamel surface.

Odontoblasts started to differentiate and secreting dentin from a distance as tooth Figure 4.13.f.

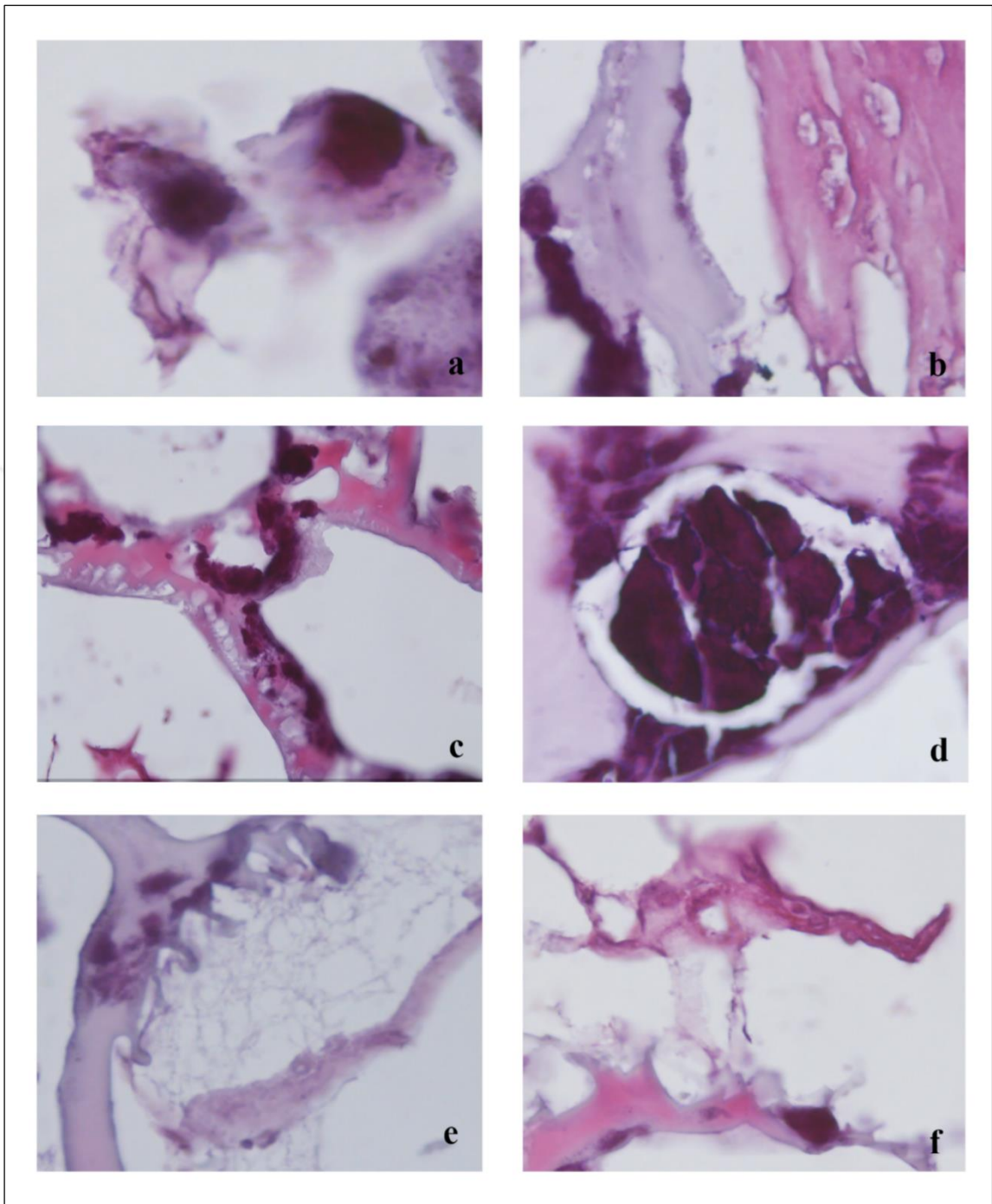


Figure 4.13. Specilized structures of cells seeded on HA hybrid scaffolds for 8 week.

4.3.3. Immunohistochemical Analysis

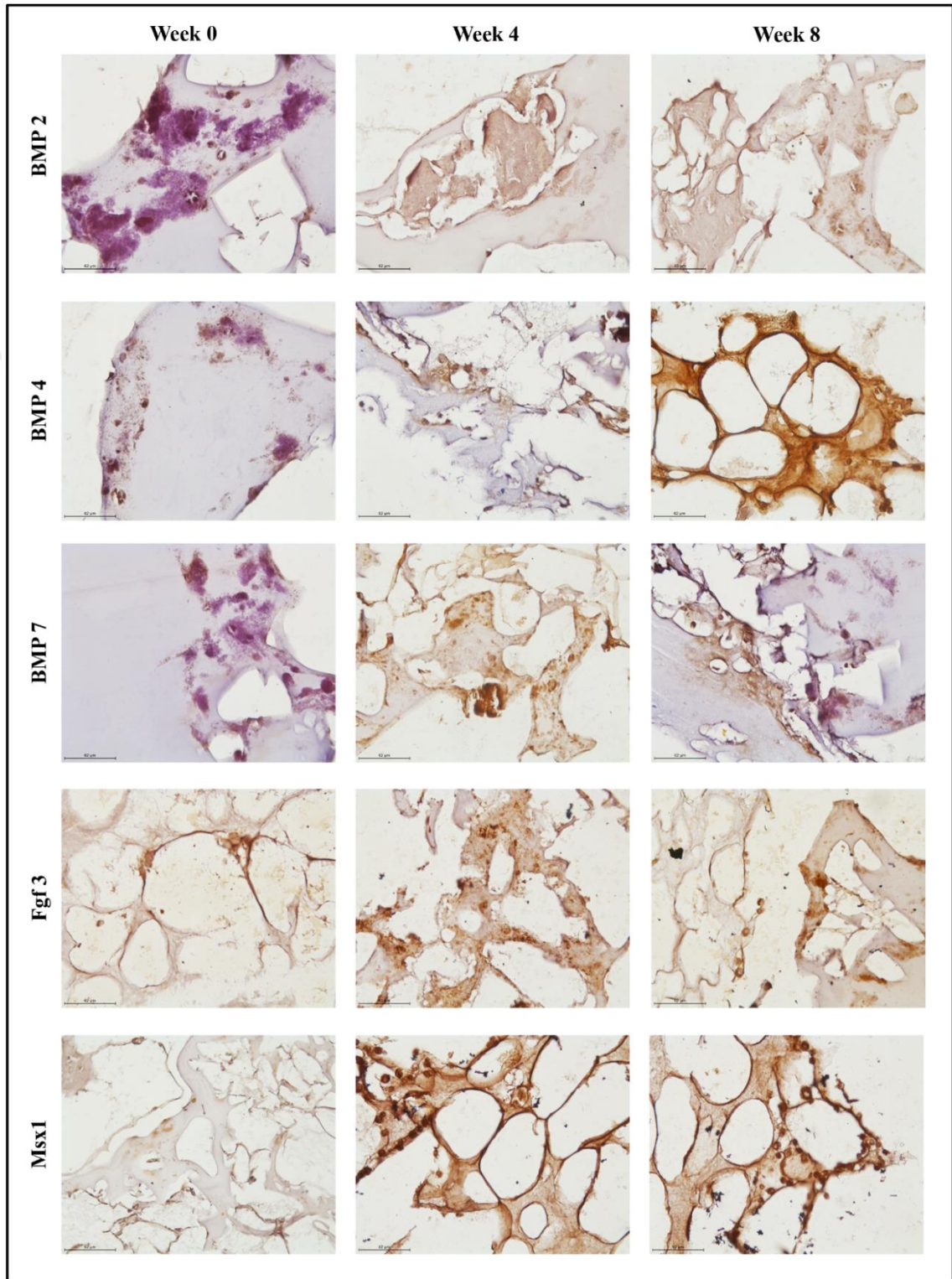


Figure 4.14. Time dependent immunohistochemical staining of tooth forming cells. Used antibodies are BMP 2, 4, 7, FGF 3 and Msx 1.

BMP 2, BMP 4 and BMP 7 are important players of signaling networks regulating tooth initiation and shape development. At first (Week 0) BMP 2 started to express from epithelial and tooth transform into the bell shape, the early bell stage (Week 4 and 8), BMP 2 expression had disappeared from the epithelial part and had shifted to the central cells of the dental papilla mesenchyme (Week 8). Subsequently, expression extended coronally in the dental papilla and differentiate in to odontoblasts (Figure 4.14.) Similar expression can be seen in BMP 7. Transcripts were localized transiently in both ameloblast and odontoblast parts but became weaker with advancing development.

The expression of BMP 4 disappeared from the dental epithelium with the removal of the enamel knot (Week 0 to 4), and expressed in the area between epithelium and differentiated odontoblastic cells (Week 4). At the 8 week BMP 4 expression had shifted to dental mesenchyme part. The epithelial cells showed very weak or no expression (Week 8). Msx 1 expression is basically controlled by BMP 4. Msx 1 expression was triggered at the dental mesenchyme by increment of BMP 4 expression in the dental mesenchyme cells. At the late stage of cap and early stage of tooth development enamel knot which is formed by epithelial cells, expresses the FGF 3 (Week 0). At the middle of bell stage enamel knot starts to disappear and FGF 3 expression can be determined at dental mesenchymal cells, mainly odontoblasts.

DMP 1, Amelogenin and DSPP express only mineralized tissue via differentiated cells by signal transduction between epithelial and mesenchymal cells. All three proteins were expressed at the important points such as dental mesenchymal matrix, mineralizing odontoblasts and external epithelium. Eventhough especially DMP 1 is not necessary to early tooth development (Week 0), to form mineralization and proper structure these proteins must be expressed (Week 4 to 8) (Figure 4. 15.). VEGF is a key regulator of blood vessel endothelial development. VEGFR expression was detected both dental mesenchyme and epithelium at certain shapes (blood vessels like shape) (Week 4 to 8).

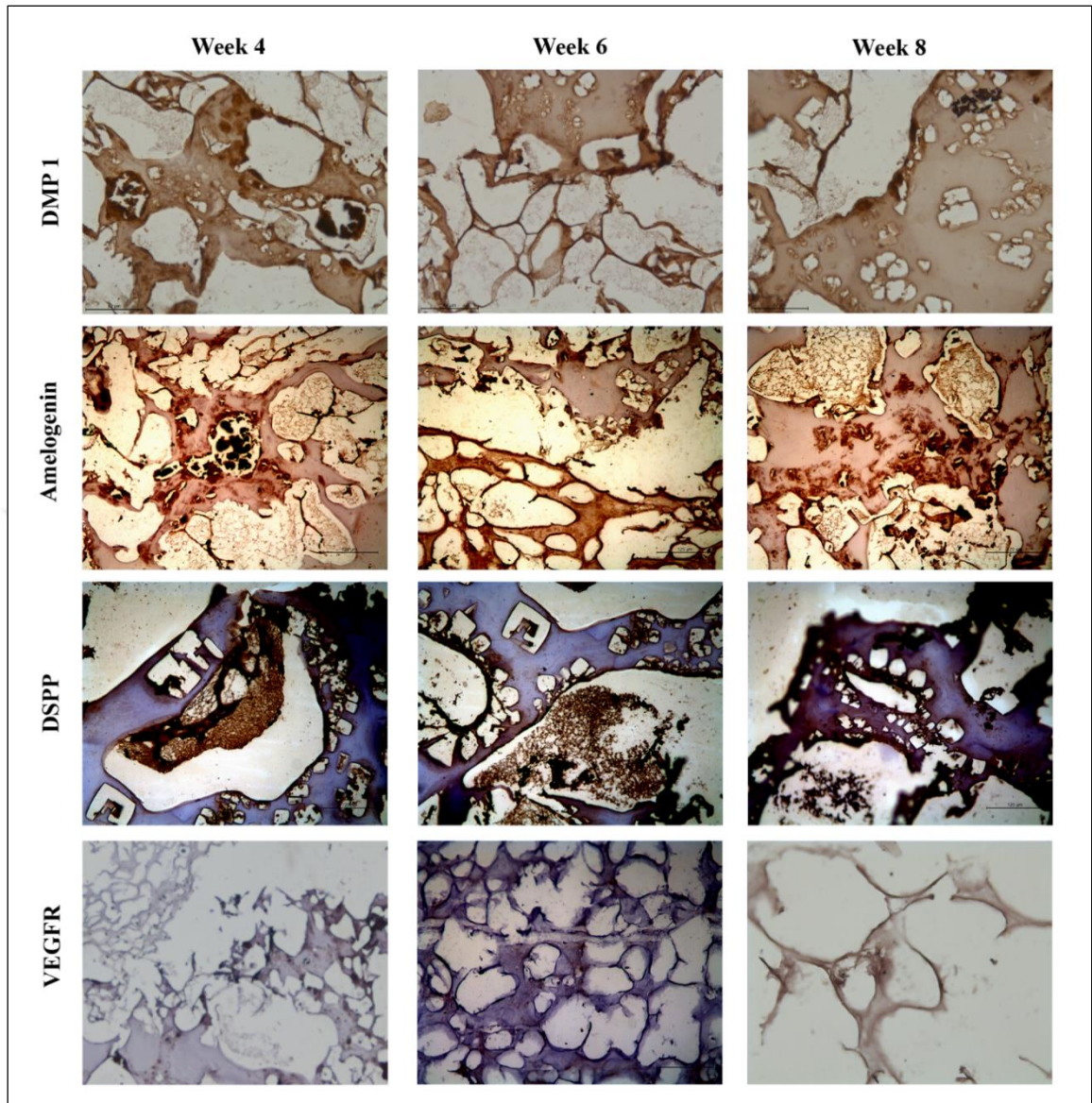


Figure 4.15. Time dependent immunohistochemical staining of tooth forming cells. Used antibodies are DMP 1, DSPP, Amelogenin and VEGFR.

5. DISCUSSION

Last decade, scientist try to understand interconnected microporous 3D HA scaffold fabrication to mimic tooth and surrounding tissue through vascularization, hard tissue growth and tissue remodeling [166-169]. One of the main approaches of hard tissue engineering are a homogenous interconnected porous structure that leads vascularization, different originated cells to form complexity of tissue and three dimensionally scaffolds which include extracellular matrix components. The gel casting method is very useble for rapidly establishing ceramic particles to get obtain interested shapes through *in situ* polymerization by which a macromolecular network is constructed to grip the ceramic particles together [169, 170].

The biochemical material used in this method is removed by biodegradation properties of cells, and the seramic particles are nontoxic to cells, allowing this materials to be used for hard tissue engineering experiments [169]. With these properties, HA scaffolds can be forming high biodegradable biomaterial and a controllable porous structure. Also, gelcasting method provides a 3D polymeric and highly porous network. Advantages of thie technique are rapidly gelation which prevents the accumulation of the blend and provide the fabrication of a homogeneous polymer matrix with equal particle dispersion, and a desirable size of macroporous HA structure. Interested size and geometries of microporous structures can be formed by desired size of NaCl particles. Figure 4.5 a and b show the porous, interconnected and uniform microstructure of HA scaffolds. The process of tooth shaped scaffold construction is shown in Figure 3.1. Mixtures of four different HA concentrations, 35, 40, 45 and 50 wt %, were prepared to understand the exact interaction of HA concentration on physical features of scaffolds. Eventhough the higher HA concentration is mandatory element for harder density of the HA scaffold, and for decreasing unnecessary mixture contraction, the high HA concentrations have a high viscosity, causing difficulty in suitable mixing and mixture dispersion. Hence, a 50 % HA particle amount was selected as the highest concentration. The right amount of monomers and HA particles (Table 4.1) were optimized to get consonant and easily handling mixture. Selecting a proper concentration of biodegradable material for the HA powder is essential to maintain a fluid blend. Colloidal examinations on HA nano powders have demonstrated that agar can be a proper agent for aqueous HA slurries [169, 171]. To prepare stable HA blend, OH groups need to be

eliminated form disintegrated structures of extra phases of calcium such as TCP, tetracalcium phosphate, and calcium oxide [172]. Eventough HA can be alter cellular response and reduce metarial biocompatibility. This biocompatibility also depends on scaffolds composition [173, 174]. The cell response against to the scaffolding material can be differ according to the calcium and phosphorous ratios, which is other calcium phosphate componouns might be harmful because of their solubility percentages and mechanical strengths [173]. Figure 4.5.a demonstrate the SEM images of the macroporous HA scaffold prepared with 40 wt % HA nano particles in the blend.

The spectrum was calculated before and after scaffolding of HA, by IR spectroscopy. According to the FTIR spectra results as shown in the Figure 4.6; two lines at 630 and 3570 cm^{-1} correspond to the vibration of OH ions, 1030 and 570 cm^{-1} are the typical lines of phosphate bending vibration, while the line at 985 cm^{-1} is known to phosphate stretching vibration. The lines at 881, 1420 and 1460 cm^{-1} are indicative of the carbonate ion substitution. The lines at 1650 and 3470 cm^{-1} correspond to H_2O absorption. The results show there was no discernible spectrum differences between HA nano particles and constructed HA scaffold lines established from the spectra, shown in the Figure 4.6 fit to HA.

Shaped scaffolds need to require to demonstrate the tooth properties not only in terms of chemical composition but also in terms of morphology. Porous structures allow development of hard and soft tissues within suitble pores and also blood supply for further vascularization and mineralization of related tissues.

SEM images in Figure 4.5 show the interconnected, macroporous composition of the HA scaffolds, which are having different pore sizes ranging from 150 to 300 μm were constructed in this study. All prepared HA scaffolds exhibited basic structural characteristics of a continuous open porous shape, with a 3D interpenetrating network of struts and pores. Eventhough Hulbert et al. demonstrated that the optimum pore size for osteoconduction is $\sim 150 \mu\text{m}$ [175], Flatley et al. shown that a pore size of $\sim 500 \mu\text{m}$ is compatible for osteoconduction [176]. Constructed pore size and an interconnecting pore structure like the ones shown in Figure 4.6 are appropriate for odontoblasts, epithelial cells and osteoblasts to expand into the scaffold pores and cavity [177] for fast vascularization, tooth generation, d,fferent types of cell interactions and remodeling [178-181]. Fast and proper vascularization and interconnected pore sturcture are necessary to form the mechanical strength and serve

as a sporting material for hard tissue because it allows secreted molecules and degraded monomers to freely exit into and out the HA scaffold.

The HA density of a porous scaffold can effect its mechanical strength, permeability, and presence of structural defects [169]. Density and porosity of HA scaffolds prepared with blend of different HA concentrations were shown in the Table 4.1. One of the challenging factor in the hard tissue engineering is identifying proper pore sizes and amount of pores which are related some functiona and physical factors such as permeability and surface area of the porous structure. High porous scaffolding with low HA concentrations gives a high surface area/volume ratio, and higher cell attachment to the scaffold and alter hard tissue regeneration but it can be cause of lower mechanical strength. On the other hand, high porosity with high HA concentrations had thicker and denser pore walls that originated from stable, non-disrupted coating and contained fewer defects, which resulted in a structure strong in mechanical strength.

Recently, tissue engineering approaches in a manner of generation and treatment of related tissues have been developed, and also bone, dental and interfacial tissue engineering prospective has gain large amount attention from scientists. Although some progress has been reported on tooth scaffolding to created dental tissues, the regeneration of certain stages of developed tooth structures remains a challenge, let alone the regeneration of the three-phase enamel-dentin-pulpa [182]. For the functional regeneration of the developed tooth constructs, different originated cells, proper extracellular matrix components, fibrous connective tissues require orientation against bone surfaces to allow optimal biomechanical integration.

In this *in vitro* study, it was shown that new methodology for cell culturing, 3D scaffolding and HA nano powder complex for tooth engineering. This controlled 3D porous structure with tissue sections that harmony the shape of anatomic immature tooth at the late bell stage with separate seeding of different originated cells by phenotype. This tooth scaffold/cell construction increased generation capacity of functional early stage of tooth within *in vitro* conditions.

For dental tissue engineering applications, it is necessary to use different cell types and proper material for induction of action in 3D scaffold and scaffold need to give easy attachment and communication with controlled engineering [169]. Additionally, coplicated 3D conditions

with unrelated chemicals, can lead to more difficult and unpredictable cell attachment, movements and even cell death. Main problem in the 3D scaffolding architecture is cell interaction with different cell types, scaffolding monomers and extra used extracellular matrix components, which are responsible for cell migration, differentiation, reorganization, vascularization and structuralization in tissue formation or wound healing [183].

Regulatory cell and tissue compartmentalization are necessary to coordinate multiple tissue complex generation and formation in a single system. Therefore, main effect such as the 3D hybrid scaffold construction increases the morphogenesis, organization, and functionalization of multiple tissue interfaces [183]. The biological contraction of dental tissues against each other was histomorphometrically observed with calcified tissue layer deposition (Figure 4.9) at 0, 4 and 8 weeks. In the microporous of HA construct, cells have ability to form tooth like structure by creating cell to cell and cell to micro environment interaction and enamel-dentin-pulpa formation, predictably and sustained over time.

The tooth model system used here allows for multi-tissue evaluation of two different mineralized structures with an intervening connected structure required for biomechanical loading and function. The advantage of this model system is that various biomechanical stimulations can be transmitted directly to just only mineralization or pulp induction. During the early stages of development of tooth, a series of specific molecules started to express including BMP 2, BMP 4, and BMP 7 are from the enamel knot which plays role as signaling center. Recent studies were shown that to show effective role of BMP 4, it was given to dental mesenchyme this lead to morphogenic changes and inducing expression of transcription factors, including Msx 1, Msx 2, Lef 1, and Egr1 in the dental mesenchyme Bmp 2, BMP 4 and BMP 7 expressed from enamel knot, may be cause for apoptosis in the knot cells at the end of the late bell stage. FGF 3 is expressed from dental mesenchyme at the bud stage and FGF 3 can stimulate the cell proliferation in isolated mesenchyme [47]. Some studies showed that FGF 3 deficient mice didn't exhibit important tooth defects [58-60]. Msx1 regulates the expression of Cbfa1/Runx2 [114, 115], while Msx1 also regulates FGF 3 expression from the dental mesenchyme [44]. So Msx 1 regulates Cbfa1/Runx2 expression controlling FGF 3 expression. All these transcription factors regulate the expression of growth factors that responsible for activation and regulation of other signaling molecules, in the developing teeth. During the mineralization stage, formation of the crown by dentinogenesis and amelogenesis with the deposition of DMP 1, DSP and COL1A (dentin

proteins) and Amelogenin (enamel protein) and the beginning of calcification are started; preameloblasts, from the inner enamel epithelium, induce adjacent cells of the dental papilla to become odontoblast that then produce the dentin matrix which in turn induces the preameloblasts to become ameloblasts that produce enamel matrix. Also, HA is representing great inductive material for hard tissue engineering. HA has high level of biocompatibility and osteoconductivity which is confirmed by OCN and SPARC protein expression levels. The identification of these proteins in the newly formed hybrid scaffold was, therefore, utilized to infer the degree of tissue maturation and stability of the developed tooth structure. Therefore, via these markers, the maturation and re-functionalization of generated dentin related organizations could be track and quantify the marker expression levels at generated regions (Figure 4.11, Figure 4.12).

The biomimetic architecture achieved here is providing a promising platform for dental tissue engineering. Besides, the microporous scaffold with certain cells can induce the functional integrity of generated dental complexes. While, main attraction of this study is the dental complex generation, the anatomical design with the internal geometries can be applied to diverse clinical applications. The current engineered hybrid scaffold system still has limitations compared to the highly complex native multi tissue formation [12,14], especially whole tooth [9,28,29]. In hard tissue engineering main challenge is the lack of a physically constructed environment as well as functional design which does not completely show the irregular and complex morphology of developed tooth [4]. Therefore, supported by the biological advantages demonstrated in this novel hybrid scaffold, a more developed tooth relevant design was constructed mimicking late bell stage of tooth to determine the ability to conform to the anatomical specifications of the tooth (Figure 4.13). The formed 3D scaffold gave internal channel structures within the dentin related structures similar tooth topology. The early stage of tooth shaped scaffold was designed to possess two separate components which are pulp as a odontogenically differentiated mesenchymal cells and dentin-enamel to make easier the assembling and adaptation through the tooth socket (Figure 4.9., 10., 11., 12). The adaptability of the constructed scaffold was evaluated by IHC analysis to establish the tooth formation. The designed dental engineered scaffold was initially conceived to increase angiogenic development and enhance biological molecule diffusivity at 4th week (Figure 4.14). This theoretical concept is supported by the *in vitro* findings, which reflect an increased number of vascular structures, enamel, dentin and mature

odontoblasts along the mineralization scaffold architecture (Figure 4.13). Many differentiated and connected cell groups especially observed at the 8th week (Figure 4.11., 12.). However, by the 8th week, a more mineralization increased level of tissue orientation as observed indifferent proportions for 4th week and 0 th week (Figure 4.9., 10., 11.). These group of cells within the scaffold were connectively localized along the tooth shaped scaffold and at the center of more mature odontoblastic structures. Together, these results support the hybrid scaffold designing with biomimetic architecture to influence cell behavior and tissue orientation. Therefore, main principal of this study is finding a combinational system of tooth (mesenchymal stem cells-epithelial cells) and odontogenic stimulation can enhance the generation of the multi layered tooth complex. According to the results, cementum, dentin, pulp and enamel like structures have found positively produced yet micro scale instead of a basic tooth regarding to the fact of the using aporous scaffold. Therefore, enamel, dentin or pulp forming structures should be unporous for tooth engineering. These findings are important as they emphasize the potential biological effect of the hybrid scaffold system.

6. CONCLUSION

A new approach combining the gel-casting method with HA-based scaffold and different cell lineages as a hybrid system leads to successively mimic the early stage of tooth development, *in vitro*. The tooth shaped constructs with a pore size ranging from 150 to 300 μm arranged by gathering right amounts of materials provide interconnected macroporous structure. Overall results showed that the scaffolding process and its product as a tooth shaped HA scaffold are suitable for cells attachment and growth which is required for effective hard tissue engineering approaches. Problems arising from a porous scaffold should be eliminated by using a system that integrates dentin and enamel uniformly instead of a porous and harsh scaffold. In conclusion, this *in vitro* study clearly demonstrates that designed 3D scaffolds shaped as a immature tooth at the late bell stage were essential to form enamel-dentin-pulp interfaces with an appropriate cell and biodegradable material combination. As a future prospect, in order to eliminate these problems, HA should be by mixed with highly collagenese gel. At the same time, those processes may be examined *in vivo* on a live organism.

REFERENCES

1. J.A. Thomson, J. Itskovitz-Eldor, S.S. Shapiro, M.A. Waknitz, J.J. Swiergiel, V.S. Marshall, and J.M. Jones. Embryonic Stem Cell Lines Derived from Human Blastocysts. *Science*. 5391:1145-1147, 1998.
2. M. Jiang, L. Lv, H. Ji, X. Yang, W. Zhu, L. Cai, X. Gu, C. Chai, S. Huang, J. Sun, and Q. Dong. Induction of Pluripotent Stem Cells Transplantation Therapy for Ischemic Stroke. *Molecular Cellular Biochemistry*. 354:1-2, 2011.
3. M. Cihova, V. Altanerova, and C. Altaner. Stem Cell Based Cancer Gene Therapy. *Molecular Pharmaceutics*. 5:1480-1487, 2011.
4. T. Yamaza, A. Kentaro, C. Chen, Y. Liu, Y. Shi, S. Gronthos, S. Wang, and S. Shi. Immunomodulatory Properties of Stem Cells from Human Exfoliated Deciduous Teeth. *Stem Cell Research and Therapy*. 1:5, 2010.
5. P.A. Zuk, M. Zhu, P. Ashjian, D.A. De Ugarte, J.I. Huang, H. Mizuno, Z.C. Alfonso, J.K. Fraser, P. Benhaim, and M.H. Hedrick. Human Adipose Tissue Is A Source of Multipotent Stem Cells. *Molecular Biology of the Cell*. 12:4279-4295, 2002.
6. F. Djouad, C. Bouffi, S. Ghannam, D. Noel, and C. Jorgensen. Mesenchymal Stem Cells: Innovative Therapeutic Tools for Rheumatic Diseases. *Nature Reviews Rheumatology*. 7:392-399, 2009.
7. A.I. Caplan and D. Correa. The MSC: An Injury Drugstore. *Cell Stem Cell*. 1:11-15, 2011.
8. A.J. Friedenstein, R.K. Chailakhjan, and K.S. Lalykina. The Development of Fibroblast Colonies In Monolayer Cultures of Guinea-Pig Bone Marrow and Spleen Cells. *Cell and Tissue Kinetics*. 4:393-403, 1970.

9. A. Alhadlaq and J.J. Mao. Tissue-Engineered Neogenesis of Human-Shaped Mandibular Condyle from Rat Mesenchymal Stem Cells. *Journal of Dental Research*. 12:951-956, 2003.
10. B.M. Thomson, J. Bennett, V. Dean, J. Triffitt, M.C. Meikle, and N. Loveridge. Preliminary Characterization of Porcine Bone Marrow Stromal Cells: Skeletogenic Potential, Colony-Forming Activity, and Response to Dexamethasone, Transforming Growth Factor Beta, and Basic Fibroblast Growth Factor. *Journal of Bone and Mineral Research*. 10:1173-1183, 1993.
11. M.F. Pittenger, A.M. Mackay, S.C. Beck, R.K. Jaiswal, R. Douglas, J.D. Mosca, M.A. Moorman, D.W. Simonetti, S. Craig, and D.R. Marshak. Multilineage Potential of Adult Human Mesenchymal Stem Cells. *Science*. 541:143-147, 1999.
12. R. Huss. Perspectives on The Morphology and Biology of CD34-Negative Stem Cells. *Journal of Hematotherapy and Stem Cell Research*. 6:783-793, 2000.
13. M. Hristov, W. Erl, and P.C. Weber. Endothelial Progenitor Cells: Isolation and Characterization. *Trends in Cardiovascular Medicine*. 5:201-205, 2003.
14. B. Seshi, S. Kumar, and D. Sellers. Human Bone Marrow Stromal Cell: Coexpression of Markers Specific for Multiple Mesenchymal Cell Lineages. *Blood Cells, Molecules and Diseases*. 3:234-246, 2000.
15. T. Kinnaird, E. Stabile, M.S. Burnett, C.W. Lee, S. Barr, S. Fuchs, and S.E. Epstein. Marrow-Derived Stromal Cells Express Genes Encoding A Broad Spectrum of Arteriogenic Cytokines and Promote In Vitro and In Vivo Arteriogenesis Through Paracrine Mechanisms. *Circulation Research*. 5:678-685, 2004.
16. K. Le Blanc, I. Rasmusson, B. Sundberg, C. Gotherstrom, M. Hassan, M. Uzunel, and O. Ringden. Treatment of Severe Acute Graft-Versus-Host Disease with Third Party Haploidentical Mesenchymal Stem Cells. *The Lancet*. 9419:1439-1441, 2004.

17. E. Zappia, S. Casazza, E. Pedemonte, F. Benvenuto, I. Bonanni, E. Gerdoni, D. Giunti, A. Ceravolo, F. Cazzanti, F. Frassoni, G. Mancardi, and A. Uccelli. Mesenchymal Stem Cells Ameliorate Experimental Autoimmune Encephalomyelitis Inducing T-Cell Anergy. *Blood*. 5:1755-1761, 2005.
18. H. Hauner and G. Loffler. Adipose tissue development: the role of precursor cells and adipogenic factors. Part I: Adipose Tissue Development and The Role of Precursor Cells. *Klinische Wochenschrift*. 17:803-811, 1987.
19. A.E. Grigoriadis, J.N. Heersche, and J.E. Aubin. Differentiation of Muscle, Fat, Cartilage, and Bone from Progenitor Cells Present in A Bone-Derived Clonal Cell Population: Effect of Dexamethasone. *Journal of Cellular Biology*. 6:2139-2151, 1988.
20. S. Wakitani, T. Saito, and A.I. Caplan. Myogenic Cells Derived from Rat Bone Marrow Mesenchymal Stem Cells Exposed to 5-Azacytidine. *Muscle and Nerve*. 12:1417-1426, 1995.
21. D. Benayahu, Y. Kletter, D. Zipori, and S. Wientroub. Bone Marrow-Derived Stromal Cell Line Expressing Osteoblastic Phenotype In Vitro and Osteogenic Capacity In Vivo. *Journal of Cellular Physiology*. 1:1-7, 1989.
22. S.P. Bruder, K.H. Kraus, V.M. Goldberg, and S. Kadiyala. The Effect of Implants Loaded with Autologous Mesenchymal Stem Cells on The Healing of Canine Segmental Bone Defects. *Journal of Bone and Joint Surgery American*. 7:985-986, 1998.
23. J.B. Gurdon. The Generation of Diversity and Pattern in Animal Development. *Cell*. 2:185-199, 1992.
24. I. Thesleff, A. Vaahtokari, and A.M. Partanen. Regulation of Organogenesis. Common Molecular Mechanisms Regulating The Development of Teeth and Other Organs. *International Journal of Developmental Biology*. 1:35-50, 1995.

25. Y.D. Zhang, Z. Chen, Y.Q. Song, C. Liu, and Y.P. Chen. Making A Tooth: Growth Factors, Transcription Factors, and Stem Cells. *Cell Research*. 5:301-316, 2005.
26. A. Alhadlaq and J.J. Mao. Mesenchymal Stem Cells: Isolation and Therapeutics. *Stem Developmental Cell* 4:436-448, 2004.
27. I. Thesleff and P. Nieminen. Tooth Morphogenesis and Cell Differentiation. *Current Opinion in Cell Biology*. 6:844-850, 1996.
28. I. Thesleff and M. Mikkola. The Role of Growth Factors in Tooth Development. *International Review of Cytology*. 217:93-135, 2002.
29. W.E. Koch. In Vitro Differentiation of Tooth Rudiments of Embryonic Mice. I. Transfilter Interaction of Embryonic Incisor Tissues. *Journal of Experimental Zoology*. 2:155-169, 1967.
30. J. Jernvall and I. Thesleff. Reiterative Signaling and Patterning During Mammalian Tooth Morphogenesis. *Mechanisms of Development*. 1:19-29, 2000.
31. A. Neubuser, H. Peters, R. Balling, and G.R. Martin. Antagonistic Interactions Between FGF and BMP Signaling Pathways: A Mechanism for Positioning The Sites of Tooth Formation. *Cell*. 2:247-25, 1997.
32. A.S. Tucker, K.L. Matthews, and P.T. Sharpe. Transformation of Tooth Type Induced by Inhibition of BMP Signaling. *Science*. 5391:1136-1138, 1998.
33. H. Peters and R. Balling. Teeth. Where and How to Make Them. *Trends in Genetics*. 2:59-65, 1999.
34. T.R. St Amand, Y. Zhang, E.V. Semina, X. Zhao, Y. Hu, L. Nguyen, J.C. Murray, and Y. Chen. Antagonistic Signals Between BMP4 and FGF8 Define The Expression of Pitx1 and Pitx2 in Mouse Tooth-Forming Anlage. *Developmental Biology*. 2:323-332, 2000.

35. J.P. Tissier-Seta, M.L. Mucchielli, M. Mark, M.G. Mattei, C. Goridis, and J.F. Brunet. Barx1, A New Mouse Homeodomain Transcription Factor Expressed in Cranio-Facial Ectomesenchyme and The Stomach. *Mechanisms of Development*. 1:3-15, 1995.
36. T.A. Mitsiadis, I. Angeli, C. James, U. Lendahl, and P.T. Sharpe. Role of Islet1 in The Patterning of Murine Dentition. *Development*. 18:4451-4460, 2003.
37. S. Vainio, I. Karavanova, A. Jowett, and I. Thesleff. Identification of BMP-4 as A Signal Mediating Secondary Induction Between Epithelial and Mesenchymal Tissues During Early Tooth Development. *Cell*. 1:45-58, 1993.
38. M.J. Bitgood and A.P. McMahon. Hedgehog and Bmp Genes Are Coexpressed at Many Diverse Sites of Cell-Cell Interaction in The Mouse Embryo. *Developmental Biology*. 1:126-138, 1995.
39. Z. Hardcastle, R. Mo, C.C. Hui, and P.T. Sharpe. The Shh Signalling Pathway in Tooth Development: Defects in Gli2 and Gli3 Mutants. *Development*. 15:2803-2811, 1998.
40. P. Kettunen and I. Thesleff. Expression and Function of FGFs-4, -8, and -9 Suggest Functional Redundancy and Repetitive Use as Epithelial Signals During Tooth Morphogenesis. *Developmental Dynamics*. 3:256-268, 1998.
41. Y. Zhang, X. Zhao, Y. Hu, T. St Amand, M. Zhang, R. Ramamurthy, M. Qiu, and Y. Chen. Msx1 Is Required for The Induction of Patched by Sonic Hedgehog in The Mammalian Tooth Germ. *Developmental Dynamics*. 1:45-53, 1999.
42. Y. Chen, M. Bei, I. Woo, I. Satokata, and R. Maas. Msx1 controls inductive signaling in mammalian tooth morphogenesis. *Development*. 10:3035-3044, 1996.

43. K. Kratochwil, M. Dull, I. Farinas, J. Galceran, and R. Grosschedl. Lef1 Expression Is Activated by BMP-4 and Regulates Inductive Tissue Interactions in Tooth and Hair Development. *Genes and Development*. 11:1382-1394, 1996.
44. M. Bei and R. Maas. FGFs and BMP4 Induce both Msx1-Independent and Msx1-Dependent Signaling Pathways in Early Tooth Development. *Development*. 21:4325-4333, 1998.
45. C.A. Ferguson, A.S. Tucker, L. Christensen, A.L. Lau, M.M. Matzuk, and P.T. Sharpe. Activin Is an Essential Early Mesenchymal Signal in Tooth Development That Is Required for Patterning of The Murine Dentition. *Genes and Development*. 16:2636-2649, 1998.
46. L. Sarkar and P.T. Sharpe. Expression of Wnt Signalling Pathway Genes During Tooth Development. *Mechanism of Development*. 1:197-200, 1999.
47. P. Kettunen, J. Laurikkala, P. Itaranta, S. Vainio, N. Itoh, and I. Thesleff. Associations of FGF-3 and FGF-10 with Signaling Networks Regulating Tooth Morphogenesis. *Developmental Dynamics*. 3:322-332, 2000.
48. J. Jernvall, T. Aberg, P. Kettunen, S. Keranen, and I. Thesleff. The Life History of An Embryonic Signaling Center: BMP-4 Induces P21 and Is Associated with Apoptosis in The Mouse Tooth Enamel Knot. *Development*. 2:161-169, 1998.
49. Y. Zhang, Z. Zhang, X. Zhao, X. Yu, Y. Hu, B. Geronimo, S.H. Fromm, and Y.P. Chen. A New Function of BMP4: Dual Role for BMP4 in Regulation of Sonic Hedgehog Expression in The Mouse Tooth Germ. *Development*. 7:1431-1443, 2000.
50. B.L. Hogan. Bone Morphogenetic Proteins: Multifunctional Regulators of Vertebrate Development. *Genes and Development*. 13:1580-1594, 1996.
51. M. Whitman. Smads and Early Developmental Signaling by The TGFbeta Superfamily. *Genes and Development*. 16:2445-2462, 1998.

52. P. ten Dijke, H. Yamashita, T.K. Sampath, A.H. Reddi, M. Estevez, D.L. Riddle, H. Ichijo, C.H. Heldin, and K. Miyazono. Identification of Type I Receptors for Osteogenic Protein-1 and Bone Morphogenetic Protein-4. *Journal of Biological Chemistry*. 25:16985-16988, 1994.
53. Y. Mishina, A. Suzuki, N. Ueno, and R.R. Behringer. Bmpr Encodes A Type I Bone Morphogenetic Protein Receptor That Is Essential for Gastrulation During Mouse Embryogenesis. *Genes and Development*. 24:3027-2037, 1995.
54. S.T. Baur, J.J. Mai, and S.M. Dymecki. Combinatorial Signaling Through BMP Receptor IB and GDF5: Shaping of The Distal Mouse Limb and The Genetics of Distal Limb Diversity. *Development*. 3:605-619, 2000.
55. S.E. Yi, A. Daluiski, R. Pederson, V. Rosen, and K.M. Lyons. The Type I BMP Receptor BMPRIIB Is Required for Chondrogenesis in The Mouse Limb. *Development*. 3:621-630, 2000.
56. J. Jernvall, P. Kettunen, I. Karavanova, L.B. Martin, and I. Thesleff. Evidence for The Role of The Enamel Knot as A Control Center in Mammalian Tooth Cusp Formation: Non-Dividing Cells Express Growth Stimulating Fgf-4 Gene. *International Journal of Developmental Biology*. 3:463-463, 1994.
57. K. Kratochwil, J. Galceran, S. Tontsch, W. Roth, and R. Grosschedl. FGF4, A Direct Target Of LEF1 and Wnt Signaling, Can Rescue The Arrest of Tooth Organogenesis in Lef1(-/-) Mice. *Genes and Development*. 24:3173-3185, 2002.
58. S.L. Mansour, J.M. Goddard, and M.R. Capecchi. Mice Homozygous for A Targeted Disruption of The Proto-Oncogene Int-2 Have Developmental Defects in The Tail and Inner Ear. *Development*. 1:13-28, 1993.
59. H. Min, D.M. Danilenko, S.A. Scully, B. Bolon, B.D. Ring, J.E. Tarpley, M. DeRose, and W.S. Simonet. Fgf-10 Is Required for Both Limb and Lung Development and

- Exhibits Striking Functional Similarity to *Drosophila* Branchless. *Genes and Development*. 20:3156-3161, 1998.
60. K. Sekine, H. Ohuchi, M. Fujiwara, M. Yamasaki, T. Yoshizawa, T. Sato, N. Yagishita, D. Matsui, Y. Koga, N. Itoh, and S. Kato. Fgf10 Is Essential for Limb and Lung Formation. *Nature Genetics*. 1:138-141, 1999.
61. A. Vaahtokari, T. Aberg, J. Jernvall, S. Keranen, and I. Thesleff. The Enamel Knot as A Signaling Center in The Developing Mouse Tooth. *Mechanisms of Development*. 1:39-43, 1996.
62. H.R. Dassule, P. Lewis, M. Bei, R. Maas, and A.P. McMahon. Sonic Hedgehog Regulates Growth and Morphogenesis of The Tooth. *Development*. 22:4775-4785, 2000.
63. A. Gritli-Linde, P. Lewis, A.P. McMahon, and A. Linde. The Whereabouts of A Morphogen: Direct Evidence for Short- and Graded Long-Range Activity of Hedgehog Signaling Peptides. *Developmental Biology*. 2:364-386, 2001.
64. M.T. Cobourne, Z. Hardcastle, and P.T. Sharpe. Sonic Hedgehog Regulates Epithelial Proliferation and Cell Survival in The Developing Tooth Germ. *Journal of Dental Research*. 11:1974-1979, 2001.
65. E. Koyama, T. Yamaai, S. Iseki, H. Ohuchi, T. Nohno, H. Yoshioka, Y. Hayashi, J.L. Leatherman, E.B. Golden, S. Noji, and M. Pacifici. Polarizing Activity, Sonic Hedgehog, and Tooth Development in Embryonic and Postnatal Mouse. *Developmental Dynamics*. 1:59-72, 1996.
66. A. Gritli-Linde, M. Bei, R. Maas, X.M. Zhang, A. Linde, and A.P. McMahon. Shh Signaling Within The Dental Epithelium Is Necessary for Cell Proliferation, Growth and Polarization. *Development*. 23:5323-5337, 2002.

67. K.M. Cadigan and R. Nusse. Wnt Signaling: A Common Theme in Animal Development. *Genes and Development*. 24:3286-3305, 1997.
68. P. Bhanot, M. Brink, C.H. Samos, J.C. Hsieh, Y. Wang, J.P. Macke, D. Andrew, J. Nathans, and R. Nusse. A New Member of The Frizzled Family from Drosophila Functions as A Wingless Receptor. *Nature*. 6588:225-230, 1996.
69. J. Yang-Snyder, J.R. Miller, J.D. Brown, C.J. Lai, and R.T. Moon. A Frizzled Homolog Functions in A Vertebrate Wnt Signaling Pathway. *Current Biology*. 10:1302-1306, 1996.
70. X. He, J.P. Saint-Jeannet, Y. Wang, J. Nathans, I. Dawid, and H. Varmus. A Member of The Frizzled Protein Family Mediating Axis Induction by Wnt-5A. *Science*. 5306:1652-1654, 1997.
71. K. Tamai, M. Semenov, Y. Kato, R. Spokony, C. Liu, Y. Katsuyama, F. Hess, J.P. Saint-Jeannet, and X. He. LDL-Receptor-Related Proteins in Wnt Signal Transduction. *Nature*. 6803:530-535, 2000.
72. K.I. Pinson, J. Brennan, S. Monkley, B.J. Avery, and W.C. Skarnes. An LDL-Receptor-Related Protein Mediates Wnt Signalling in Mice. *Nature*. 6803:535-538, 2000.
73. A.M. Zorn. Wnt Signalling: Antagonistic Dickkopfs. *Current Biology*. 15:R592-R595, 2001.
74. A. Rattner, J.C. Hsieh, P.M. Smallwood, D.J. Gilbert, N.G. Copeland, N.A. Jenkins, and J. Nathans. A Family of Secreted Proteins Contains Homology to The Cysteine-Rich Ligand-Binding Domain of Frizzled Receptors. *Proceedings of the National Academy of Sciences U S A*. 7:2859-2863, 1997.

75. L. Leyns, T. Bouwmeester, S.H. Kim, S. Piccolo, and E.M. De Robertis. Frzb-1 Is A Secreted Antagonist of Wnt Signaling Expressed in The Spemann Organizer. *Cell*. 6:747-756, 1997.
76. R.T. Moon, J.D. Brown, J.A. Yang-Snyder, and J.R. Miller. Structurally Related Receptors and Antagonists Compete for Secreted Wnt Ligands. *Cell*. 6:725-728, 1997.
77. L. Sarkar, M. Cobourne, S. Naylor, M. Smalley, T. Dale, and P.T. Sharpe. Wnt/Shh Interactions Regulate Ectodermal Boundary Formation During Mammalian Tooth Development. *Proceedings of the National Academy of Sciences U S A*. 9:4520-4524, 2000.
78. H.R. Dassule and A.P. McMahon. Analysis of Epithelial-Mesenchymal Interactions in The Initial Morphogenesis of The Mammalian Tooth. *Developmental Biology*. 2:215-227, 1998.
79. C. van Genderen, R.M. Okamura, I. Farinas, R.G. Quo, T.G. Parslow, L. Bruhn, and R. Grosschedl. Development of Several Organs That Require Inductive Epithelial-Mesenchymal Interactions Is Impaired in LEF-1-Deficient Mice. *Genes and Development*. 22:2691-2703, 1994.
80. L. Sarkar and P.T. Sharpe. Inhibition of Wnt Signaling by Exogenous Mfrzb1 Protein Affects Molar Tooth Size. *Journal of Dental Research*. 4:920-925, 2000.
81. S.E. Millar, E. Koyama, S.T. Reddy, T. Andl, T. Gaddapara, R. Piddington, and C.W. Gibson. Over- and Ectopic Expression of Wnt3 Causes Progressive Loss of Ameloblasts in Postnatal Mouse Incisor Teeth. *Connective Tissue Research*. 1:121-129, 2003.
82. P. Liu, M. Wakamiya, M.J. Shea, U. Albrecht, R.R. Behringer, and A. Bradley. Requirement for Wnt3 in Vertebrate Axis Formation. *Nature Genetics*. 4:361-365, 1999.

83. T.P. Yamaguchi, A. Bradley, A.P. McMahon, and S. Jones. A Wnt5a Pathway Underlies Outgrowth of Multiple Structures in The Vertebrate Embryo. *Development*. 6:1211-1223, 1999.
84. D.S. Falconer. A Totally Sex-Linked Gene in The House Mouse. *Nature*. 4303:664-665, 1952.
85. J. Pispa, H.S. Jung, J. Jernvall, P. Kettunen, T. Mustonen, M.J. Tabata, J. Kere, and I. Thesleff. Cusp Patterning Defect in Tabby Mouse Teeth and Its Partial Rescue by FGF. *Developmental Biology*. 2:521-534, 1999.
86. H. Gruneberg. Genes and Genotypes Affecting The Teeth of The Mouse. *Journal of Embryology and Experimental Morphology*. 2:137-59, 1965.
87. J.A. Sofaer. The Teeth of The "Sleek" Mouse. *Archives of Oral Biology*. 4:299-301, 1977.
88. J. Laurikkala, M. Mikkola, T. Mustonen, T. Aberg, P. Koppinen, J. Pispa, P. Nieminen, J. Galceran, R. Grosschedl, and I. Thesleff. TNF Signaling Via The Ligand-Receptor Pair Ectodysplasin And Edar Controls The Function of Epithelial Signaling Centers and Is Regulated by Wnt and Activin During Tooth Organogenesis. *Developmental Biology*. 2:443-455, 2001.
89. J. Kere, A.K. Srivastava, O. Montonen, J. Zonana, N. Thomas, B. Ferguson, F. Munoz, D. Morgan, A. Clarke, P. Baybayan, E.Y. Chen, S. Ezer, U. Saarialho-Kere, A. de la Chapelle, and D. Schlessinger. X-linked Anhidrotic (Hypohidrotic) Ectodermal Dysplasia Is Caused by Mutation in A Novel Transmembrane Protein. *Nature Genetics*. 4:409-416, 1996.
90. A.S. Tucker, D.J. Headon, P. Schneider, B.M. Ferguson, P. Overbeek, J. Tschopp, and P.T. Sharpe. Edar/Eda Interactions Regulate Enamel Knot Formation in Tooth Morphogenesis. *Development*. 21:4691-4700, 2000.

91. D.J. Headon, S.A. Emmal, B.M. Ferguson, A.S. Tucker, M.J. Justice, P.T. Sharpe, J. Zonana, and P.A. Overbeek. Gene Defect in Ectodermal Dysplasia Implicates A Death Domain Adapter in Development. *Nature*. 6866:913-916, 2001.
92. O. Elomaa, K. Pulkkinen, U. Hannelius, M. Mikkola, U. Saarialho-Kere, and J. Kere. Ectodysplasin Is Released by Proteolytic Shedding and Binds to The EDAR Protein. *Human Molecular Genetics*. 9:953-962, 2001.
93. O. Gaide and P. Schneider. Permanent Correction of An Inherited Ectodermal Dysplasia with Recombinant EDA. *Nature Medicine*. 5:614-618, 2003.
94. A.S. Tucker, D.J. Headon, J.M. Courtney, P. Overbeek, and P.T. Sharpe. The Activation Level of The TNF Family Receptor, Edar, Determines Cusp Number and Tooth Number During Tooth Development. *Developmental Biology*. 1:185-194, 2004.
95. A.T. Kangas, A.R. Evans, I. Thesleff, and J. Jernvall. Nonindependence of Mammalian Dental Characters. *Nature*. 7014:211-214, 2004.
96. M. Yan, L.C. Wang, S.G. Hymowitz, S. Schilbach, J. Lee, A. Goddard, A.M. de Vos, W.Q. Gao, and V.M. Dixit. Two-Amino Acid Molecular Switch in An Epithelial Morphogen That Regulates Binding to Two Distinct Receptors. *Science*. 5491:523-527, 2000.
97. R. Doffinger, A. Smahi, C. Bessia, F. Geissmann, J. Feinberg, A. Durandy, C. Bodemer, S. Kenwrick, S. Dupuis-Girod, S. Blanche, P. Wood, S.H. Rabia, D.J. Headon, P.A. Overbeek, F. Le Deist, S.M. Holland, K. Belani, D.S. Kumararatne, A. Fischer, R. Shapiro, M.E. Conley, E. Reimund, H. Kalhoff, M. Abinun, A. Munnich, A. Israel, G. Courtois, and J.L. Casanova. X-Linked Anhidrotic Ectodermal Dysplasia with Immunodeficiency Is Caused by Impaired NF-Kappab Signaling. *Nature Genetics*. 3:277-285, 2001.

98. P. Koppinen, J. Pispä, J. Laurikkala, I. Thesleff, and M.L. Mikkola. Signaling and subcellular localization of the TNF receptor Edar. *Experimental Cell Research*. 2:277-285, 2001.
99. A. Ohazama, Y. Hu, R. Schmidt-Ullrich, Y. Cao, C. Scheidereit, M. Karin, and P.T. Sharpe. A Dual Role for Ikk Alpha in Tooth Development. *Developmental Cell*. 2:219-227, 2004.
100. A. Ohazama, J.M. Courtney, A.S. Tucker, A. Naito, S. Tanaka, J. Inoue, and P.T. Sharpe. Traf6 Is Essential for Murine Tooth Cusp Morphogenesis. *Developmental Dynamics*. 1:131-135, 2004.
101. A. Ohazama, J.M. Courtney, and P.T. Sharpe. Expression of TNF-Receptor-Associated Factor Genes in Murine Tooth Development. *Gene Exprimental Patterns*. 2:127-129, 2003.
102. G. Townsend, E.F. Harris, H. Lesot, F. Clauss, and A. Brook. Morphogenetic Fields Within The Human Dentition: A New, Clinically Relevant Synthesis of An Old Concept. *Archives of Oral Biology*. 1:S34-S44, 2009.
103. B.L. Thomas, A.S. Tucker, M. Qui, C.A. Ferguson, Z. Hardcastle, J.L. Rubenstein, and P.T. Sharpe. Role of Dlx-1 And Dlx-2 Genes in Patterning of The Murine Dentition. *Development*. 23:4811-4818, 1997.
104. A. Mackenzie, G.L. Leeming, A.K. Jowett, M.W. Ferguson, and P.T. Sharpe. The Homeobox Gene Hox 7.1 Has Specific Regional and Temporal Expression Patterns During Early Murine Craniofacial Embryogenesis, Especially Tooth Development In Vivo and In Vitro. *Development*. 2:269-285, 1991.
105. I. Satokata and R. Maas. Msx1 Deficient Mice Exhibit Cleft Palate and Abnormalities of Craniofacial and Tooth Development. *Nature Genetics*. 4:348-356, 1994.

106. I. Satokata, L. Ma, H. Ohshima, M. Bei, I. Woo, K. Nishizawa, T. Maeda, Y. Takano, M. Uchiyama, S. Heaney, H. Peters, Z. Tang, R. Maxson, and R. Maas. *Msx2* Deficiency in Mice Causes Pleiotropic Defects in Bone Growth and Ectodermal Organ Formation. *Nature Genetics*. 4:391-395, 2000.
107. M. Bei, K. Kratochwil, and R.L. Maas. BMP4 Rescues A Non-Cell-Autonomous Function of *Msx1* in Tooth Development. *Development*. 21:4711-4718, 2000.
108. H. Peters, A. Neubuser, K. Kratochwil, and R. Balling. Pax9-Deficient Mice Lack Pharyngeal Pouch Derivatives and Teeth and Exhibit Craniofacial and Limb Abnormalities. *Genes and Development*. 17:2735-2747, 1998.
109. E.V. Semina, R. Reiter, N.J. Leysens, W.L. Alward, K.W. Small, N.A. Datson, J. Siegel-Bartelt, D. Bierke-Nelson, P. Bitoun, B.U. Zabel, J.C. Carey, and J.C. Murray. Cloning and Characterization of A Novel Bicoid-Related Homeobox Transcription Factor Gene, RIEG, Involved in Rieger Syndrome. *Nature Genetics*. 4:1-11, 1996.
110. C.R. Lin, C. Kioussi, S. O'Connell, P. Briata, D. Szeto, F. Liu, J.C. Izpisua-Belmonte, and M.G. Rosenfeld. *Pitx2* Regulates Lung Asymmetry, Cardiac Positioning and Pituitary and Tooth Morphogenesis. *Nature*. 6750:279-282, 1999.
111. W. Liu, J. Selever, M.F. Lu, and J.F. Martin. Genetic Dissection Of *Pitx2* In Craniofacial Development Uncovers New Functions in Branchial Arch Morphogenesis, Late Aspects of Tooth Morphogenesis and Cell Migration. *Development*. 25:6375-6385, 2003.
112. P. Ducy. *Cbfa1*: A Molecular Switch in Osteoblast Biology. *Developmental Dynamics*. 4:461-471, 2000.
113. R.N. D'Souza, T. Aberg, J. Gaikwad, A. Cavender, M. Owen, G. Karsenty, and I. Thesleff. *Cbfa1* Is Required for Epithelial-Mesenchymal Interactions Regulating Tooth Development in Mice. *Development*. 13:2911-2920, 1999.

114. T. Aberg, X.P. Wang, J.H. Kim, T. Yamashiro, M. Bei, R. Rice, H.M. Ryoo, and I. Thesleff. Runx2 Mediates FGF Signaling from Epithelium to Mesenchyme During Tooth Morphogenesis. *Developmental Biology*. 1:76-91, 2004.
115. Z. Zhang, Y. Song, X. Zhang, J. Tang, J. Chen, and Y. Chen. Msx1/Bmp4 Genetic Pathway Regulates Mammalian Alveolar Bone Formation Via Induction Of Dlx5 and Cbfa1. *Mechanism of Development*. 12:1469-1479, 2003.
116. P. Bianco and P.G. Robey. Stem Cells in Tissue Engineering. *Nature*. 6859:118-121, 2001.
117. I. Thesleff and P. Sharpe. Signalling Networks Regulating Dental Development. *Mechanism of Development*. 2:111-123, 1997.
118. A.A. Volponi, Y. Pang, and P.T. Sharpe. Stem Cell-Based Biological Tooth Repair and Regeneration. *Trends in Cellular Biology*. 12:715-722, 2010.
119. J.C. Brodie and H.D. Humes. Stem Cell Approaches for The Treatment of Renal Failure. *Pharmacological Reviews*. 3:299-313, 2005.
120. S.P. Medvedev, A.I. Shevchenko, and S.M. Zakian. Induced Pluripotent Stem Cells: Problems and Advantages When Applying Them in Regenerative Medicine. *Acta Naturae*. 2:18, 2010.
121. M. Arakaki, M. Ishikawa, T. Nakamura, T. Iwamoto, A. Yamada, E. Fukumoto, M. Saito, K. Otsu, H. Harada, Y. Yamada, and S. Fukumoto. Role of Epithelial-Stem Cell Interactions During Dental Cell Differentiation. *Journal of Biological Chemistry*. 13:10590-10601, 2012.
122. P.C. Baer and H. Geiger. Adipose-Derived Mesenchymal Stromal/Stem Cells: Tissue Localization, Characterization, and Heterogeneity. *Stem Cells International*. 2012:256-265, 2012.

123. D.L. Butler, S.A. Goldstein, and F. Guilak. Functional Tissue Engineering: The Role of Biomechanics. *Journal of Biomechanical Engineering*. 6:570-575, 2000.
124. S.P. Bruder, N. Jaiswal, N.S. Ricalton, J.D. Mosca, K.H. Kraus, and S. Kadiyala. Mesenchymal Stem Cells in Osteobiology and Applied Bone Regeneration. *Clinical Orthopaedics and Related Research*. 355:S247-S256, 1998.
125. L.A. Solchaga, J.F. Welter, D.P. Lennon, and A.I. Caplan. Generation of Pluripotent Stem Cells and Their Differentiation to The Chondrocytic Phenotype. *Methods in Molecular Medicine*. 100:53-67, 2004.
126. H. Ohgushi and A.I. Caplan. Stem Cell Technology and Bioceramics: from Cell to Gene Engineering. *Journal of Biomedical Materials Research*. 6:913-927, 1999.
127. K. Nishimura, L.A. Solchaga, A.I. Caplan, J.U. Yoo, V.M. Goldberg, and B. Johnstone. Chondroprogenitor Cells of Synovial Tissue. *Arthritis Rheumatology*. 12:2631-2637, 1999.
128. H. Ohgushi and S. Isomoto. The Effect of Growth Factors in Fracture Healing and Composite Grafts of Growth Factors and Marrow Mesenchymal Cells. *Clinical Calcium*. 10:1301-1305, 2003.
129. K.R. Kirker, Y. Luo, J.H. Nielson, J. Shelby, and G.D. Prestwich. Glycosaminoglycan Hydrogel Films as Bio-Interactive Dressings for Wound Healing. *Biomaterials*. 17:3661-3671, 2002.
130. S. Kadiyala, R.G. Young, M.A. Thiede, and S.P. Bruder. Culture Expanded Canine Mesenchymal Stem Cells Possess Osteochondrogenic Potential in Vivo and In Vitro. *Cell Transplantation*. 2:125-134, 1997.
131. B.P. Chan and K.W. Leong. Scaffolding in Tissue Engineering: General Approaches and Tissue-Specific Considerations. *European Spine Journal*. 17:467-479, 2008.

132. G.Q. Chen and Q. Wu. The Application of Polyhydroxyalkanoates as Tissue Engineering Materials. *Biomaterials*. 33:6565-6575, 2005.
133. J.C. Middleton and A.J. Tipton. Synthetic Biodegradable Polymers as Orthopedic Devices. *Biomaterials*. 23:2335-2346, 2000.
134. S. Yang, K.F. Leong, Z. Du, and C.K. Chua. The Design of Scaffolds for Use in Tissue Engineering. Part I. Traditional Factors. *Tissue Engineering*. 6:679-689, 2001.
135. P.A. Gunatillake and R. Adhikari. Biodegradable Synthetic Polymers for Tissue Engineering. *European Cells and Materials*. 5:1-16, 2003.
136. N. Zhang and D.H. Kohn. Using Polymeric Materials to Control Stem Cell Behavior for Tissue Regeneration. *Birth Defects Research Part C: Embryo Today*. 1:63-81, 2012.
137. E.J. Bergsma, F.R. Rozema, R.R. Bos, and W.C. de Bruijn. Foreign Body Reactions To Resorbable Poly(L-Lactide) Bone Plates and Screws Used for The Fixation of Unstable Zygomatic Fractures. *Journal of Oral and Maxillofacial Surgery*. 6:666-670, 1993.
138. C. Martin, H. Winet, and J.Y. Bao. Acidity Near Eroding Polylactide-Polyglycolide In Vitro and In Vivo in Rabbit Tibial Bone Chambers. *Biomaterials*. 24:2373-2380, 1996.
139. A.S. Dunn, P.G. Campbell, and K.G. Marra. The Influence of Polymer Blend Composition on The Degradation of Polymer/Hydroxyapatite Biomaterials. *Journal of Material Science and Matererial Medicine*. 8:673-677, 2001.
140. W. Heidemann, S. Jeschkeit, K. Ruffieux, J.H. Fischer, M. Wagner, G. Kruger, E. Wintermantel, and K.L. Gerlach. Degradation of Poly(D,L)Lactide Implants With or Without Addition of Calciumphosphates In Vivo. *Biomaterials*. 17:2371-2381, 2001.

141. J. Rich, T. Jaakkola, T. Tirri, T. Narhi, A. Yli-Urpo, and J. Seppala. In Vitro Evaluation of Poly(Epsilon-Caprolactone-Co-DL-Lactide)/ Bioactive Glass Composites. *Biomaterials*. 10:2143-2150, 2002.
142. G. Schmidmaier, B. Wildemann, H. Bail, M. Lucke, T. Fuchs, A. Stemberger, A. Flyvbjerg, N.P. Haas, and M. Raschke. Local Application of Growth Factors (Insulin-Like Growth Factor-1 and Transforming Growth Factor-Beta1) from A Biodegradable Poly(D,L-Lactide) Coating of Osteosynthetic Implants Accelerates Fracture Healing in Rats. *Bone*. 4:341-350, 2001.
143. H. Gollwitzer, P. Thomas, P. Diehl, E. Steinhauser, B. Summer, S. Barnstorf, L. Gerdesmeyer, W. Mittelmeier, and A. Stemberger. Biomechanical and Allergological Characteristics of A Biodegradable Poly(D,L-Lactic Acid) Coating for Orthopaedic Implants. *Journal of Orthopaedic Research*. 4:802-805, 2005.
144. C.G. Pitt, M.M. Gratzl, G.L. Kimmel, J. Surles, and A. Schindler. Aliphatic Polyesters II. The Degradation of Poly (DL-Lactide), Poly (Epsilon-Caprolactone), and Their Copolymers In Vivo. *Biomaterials*. 4:215-220, 1981.
145. K. Rezwan, Q.Z. Chen, J.J. Blaker, and A.R. Boccaccini. Biodegradable and Bioactive Porous Polymer/Inorganic Composite Scaffolds for Bone Tissue Engineering. *Biomaterials*. 18:3413-3431, 2006.
146. S.J. Peter, L. Lu, D.J. Kim, G.N. Stamatias, M.J. Miller, M.J. Yaszemski, and A.G. Mikos. Effects of Transforming Growth Factor Beta1 Released from Biodegradable Polymer Microparticles on Marrow Stromal Osteoblasts Cultured on Poly(Propylene Fumarate) Substrates. *Journal of Biomedical Materials Research*. 3:452-462, 2000.
147. Z. Chen, S. Cheng, Z. Li, K. Xu, and G.Q. Chen. Synthesis, Characterization and Cell Compatibility of Novel Poly(Ester Urethane)S Based on Poly(3-Hydroxybutyrate-Co-4-Hydroxybutyrate) and Poly(3-Hydroxybutyrate-Co-3-Hydroxyhexanoate) Prepared by Melting Polymerization. *Journal of Biomaterial Science Polymer Edition*. 10:1451-1471, 2009.

148. H. Li, R. Du, and J. Chang. Fabrication, Characterization, and In Vitro Degradation of Composite Scaffolds Based on PHBV and Bioactive Glass. *Journal of Biomaterials Applications*. 2:137-155, 2005.
149. C. Doyle, E.T. Tanner, and W. Bonfield. In Vitro and In Vivo Evaluation of Polyhydroxybutyrate and of Polyhydroxybutyrate Reinforced with Hydroxyapatite. *Biomaterials*. 9:841-847, 1991.
150. S. Verma, Y. Bhatia, S.P. Valappil, and I. Roy. A Possible Role of Poly-3-Hydroxybutyric Acid in Antibiotic Production in Streptomyces. *Archives of Microbiology*. 1:66-69, 2002.
151. L. Erdmann and K.E. Uhrich. Synthesis and Degradation Characteristics of Salicylic Acid-Derived Poly(Anhydride-Esters). *Biomaterials*. 19:1941-1946, 2000.
152. L.L. Hench. The Story of Bioglass. *Journal of Material Science: Materials in Medicine*. 11:967-978, 2006.
153. M.M. Pereira, A.E. Clark, and L.L. Hench. Calcium Phosphate Formation on Sol-Gel-Derived Bioactive Glasses In Vitro. *Journal of Biomedical Materials Research*. 6:693-698, 1994.
154. J. Wilson, G.H. Pigott, F.J. Schoen, and L.L. Hench. Toxicology and Biocompatibility of Bioglasses. *Journal of Biomedical Materials Research*. 6:805-817, 1981.
155. K.D. Lobel and L.L. Hench. In Vitro Adsorption and Activity of Enzymes on Reaction Layers of Bioactive Glass Substrates. *Journal of Biomedical Materials Research*. 4:575-579, 1998.
156. H. Ohgushi, Y. Dohi, T. Yoshikawa, S. Tamai, S. Tabata, K. Okunaga, and T. Shibuya. Osteogenic Differentiation of Cultured Marrow Stromal Stem Cells on The

- Surface of Bioactive Glass Ceramics. *Journal of Biomedical Materials Research*. 3:341-348, 1996.
157. R.M. Day, A.R. Boccaccini, S. Shurey, J.A. Roether, A. Forbes, L.L. Hench, and S.M. Gabe. Assessment of Polyglycolic Acid Mesh and Bioactive Glass for Soft-Tissue Engineering Scaffolds. *Biomaterials*. 27:5857-65866, 2004.
158. H. Keshaw, A. Forbes, and R.M. Day. Release of Angiogenic Growth Factors from Cells Encapsulated in Alginate Beads with Bioactive Glass. *Biomaterials*. 19:4171-4179, 2005.
159. E. Schepers, M. de Clercq, P. Ducheyne, and R. Kempeneers. Bioactive Glass Particulate Material as A Filler for Bone Lesions. *Journal of Oral Rehabilitation*. 5:439-452, 1991.
160. J.A. Roether, J.E. Gough, A.R. Boccaccini, L.L. Hench, V. Maquet, and R. Jerome. Novel Bioresorbable and Bioactive Composites Based on Bioactive Glass and Polylactide Foams for Bone Tissue Engineering. *Journal of Materials Science: Materials in Medicine*. 12:1207-1214, 2002.
161. I.D. Xynos, A.J. Edgar, L.D. Buttery, L.L. Hench, and J.M. Polak. Ionic Products of Bioactive Glass Dissolution Increase Proliferation of Human Osteoblasts and Induce Insulin-Like Growth Factor II Mrna Expression and Protein Synthesis. *Biochemical and Biophysiological Research Communications*. 2:461-465, 2000.
162. I.D. Xynos, M.V. Hukkanen, J.J. Batten, L.D. Buttery, L.L. Hench, and J.M. Polak. Bioglass 45S5 Stimulates Osteoblast Turnover and Enhances Bone Formation In Vitro: Implications and Applications for Bone Tissue Engineering. *Calcified Tissue International*. 4:321-329, 2000.
163. H. Oonishi, L.L. Hench, J. Wilson, F. Sugihara, E. Tsuji, M. Matsuura, S. Kin, T. Yamamoto, and S. Mizokawa. Quantitative Comparison of Bone Growth Behavior

- in Granules of Bioglass, A-W Glass-Ceramic, and Hydroxyapatite. *Journal of Biomedical Materials Research*. 1:37-46, 2000.
164. M. Jarcho, J.F. Kay, K.I. Gumaer, R.H. Doremus, and H.P. Drobeck. Tissue, Cellular and Subcellular Events at A Bone-Ceramic Hydroxylapatite Interface. *Journal of Bioscience and Bioengineering*. 2:79-92, 1977.
165. B.A. Bunnell, M. Flaat, C. Gagliardi, B. Patel, and C. Ripoll. Adipose-Derived Stem Cells: Isolation, Expansion and Differentiation. *Methods*. 2:115-120, 2008.
166. H. Ohgushi, M. Okumura, T. Yoshikawa, K. Inoue, N. Senpuku, S. Tamai, and E.C. Shors. Bone Formation Process in Porous Calcium Carbonate and Hydroxyapatite. *Journal of Biomedical Materials Research*. 7:885-895, 1992.
167. T. Yoshikawa, H. Ohgushi, and S. Tamai. Immediate Bone Forming Capability of Prefabricated Osteogenic Hydroxyapatite. *Journal of Biomedical Materials Research*. 3:491-492, 1996.
168. S.H. Li, J.R. De Wijn, P. Layrolle, and K. de Groot. Synthesis of Macroporous Hydroxyapatite Scaffolds for Bone Tissue Engineering. *Journal of Biomedical Materials Research*. 1:109-120, 2002.
169. P. Sepulveda, J.G. Binner, S.O. Rogero, O.Z. Higa, and J.C. Bressiani. Production of Porous Hydroxyapatite by The Gel-Casting of Foams and Cytotoxic Evaluation. *Journal of Biomedical Materials Research*. 1:27-34, 2000.
170. D.J. Netz, P. Sepulveda, V.C. Pandolfelli, A.C. Spadaro, J.B. Alencastre, M.V. Bentley, and J.M. Marchetti. Potential Use of Gelcasting Hydroxyapatite Porous Ceramic as An Implantable Drug Delivery System. *International Journal of Pharmaceutics*. 1:117-125, 2001.
171. L.M. Rodriguez-Lorenzo, M. Vallet-Regi, and J.M. Ferreira. Colloidal Processing of Hydroxyapatite. *Biomaterials*. 13:1847-1852, 2001.

172. A. Tampieri, G. Celotti, F. Szontagh, and E. Landi. Sintering and Characterization of HA And TCP Bioceramics with Control of Their Strength and Phase Purity. *Journal of Materials Science: Materials in Medicine*. 1:29-37, 1997.
173. S. Best, B. Sim, M. Kayser, and S. Downes. The Dependence of Osteoblastic Response on Variations in The Chemical Composition and Physical Properties of Hydroxyapatite. *Journal of Materials Science: Materials in Medicine*. 2:97-103, 1997.
174. P.S. Eggli, W. Muller, and R.K. Schenk. Porous Hydroxyapatite and Tricalcium Phosphate Cylinders with Two Different Pore Size Ranges Implanted in The Cancellous Bone of Rabbits. A Comparative Histomorphometric and Histologic Study of Bony Ingrowth and Implant Substitution. *Clinical Orthopaedics and Related Research*. 232:127-138, 1988.
175. S.F. Hulbert, S.J. Morrison, and J.J. Klawitter. Tissue Reaction to Three Ceramics of Porous And Non-Porous Structures. *Journal of Biomedical Materials Research*. 5:347-374, 1972.
176. T.J. Flatley, K.L. Lynch, and M. Benson. Tissue Response to Implants of Calcium Phosphate Ceramic in The Rabbit Spine. *Clinical Orthopaedics and Related Research*. 179:246-257, 1983.
177. S. Joschek, B. Nies, R. Krotz, and A. Goferich. Chemical and Physicochemical Characterization of Porous Hydroxyapatite Ceramics Made of Natural Bone. *Biomaterials*. 16:1645-1658, 2000.
178. H. Schliephake, F.W. Neukam, and D. Klosa. Influence of Pore Dimensions on Bone Ingrowth into Porous Hydroxylapatite Blocks Used as Bone Graft Substitutes. A Histometric Study. *International Journal of Oral Maxillofacial Surgery*. 1:53-58, 1991.

179. R.E. Holmes. Bone Regeneration Within A Coralline Hydroxyapatite Implant. *Plastic and Reconstructive Surgery*. 5:626-633, 1979.
180. G. Guillemin, A. Meunier, P. Dallant, P. Christel, J.C. Pouliquen, and L. Sedel. Comparison of Coral Resorption and Bone Apposition with Two Natural Corals of Different Porosities. *Journal of Biomedical Materials Research*. 7:765-779, 1989.
181. T.E. Gresta, J.E. Zins, and T.W. Bauer. The Rate of Vascularization of Coralline Hydroxyapatite. *Plastic and Reconstructive Surgery*. 2:245-249, 1989.
182. K. de Groot. Bioceramics Consisting of Calcium Phosphate Salts. *Biomaterials*. 1:47-50, 1980.
183. H.R. Ramay and M. Zhang. Preparation of Porous Hydroxyapatite Scaffolds by Combination of The Gel-Casting and Polymer Sponge Methods. *Biomaterials*. 19:3293-3302, 2003.